non-small-cell lung cancer patients treated with gefitinib. J Clin Oncol 24: 2549–2556.
21. Kudoh S, Kato H, Nishiwaki Y, Fukuoka M, Nakata K, et al. (2008) Interstitial lung disease in Japanese patients with lung cancer: a cohort and nested case-control study. Am J Respir Crit Care Med 177: 1348–1357.
22. Suzuki H, Aoshiba K, Yokohori N, Nagai A (2003) Epidermal growth factor receptor tyrosine kinase inhibition augments a murine model of pulmonary fibrosis. Cancer Res 63: 5054–5059.
23. Ishii Y, Fujimoto S, Fukuda T (2006) Gefitinib prevents bleomycin-induced lung fibrosis in mice. Am J Respir Crit Care Med 174: 550–556.
24. Richter K, Haslbeck M, Buchner J (2010) The heat shock response: life on the verge of death. Mol Cell 40: 253–266.
25. Mathew A, Morimoto RI (1998) Role of the heat-shock response in the life and death of proteins. Ann N Y Acad Sci 851: 99–111.
26. Hirakawa T, Rokutan K, Nikawa T, Kishi K (1996) Geranylgeranylacetone induces heat shock proteins in cultured guinea pig gastric mucosal cells and rat gastric mucosa. Gastroenterology 111: 345–357.
27. Tomisato W, Takahashi N, Komoto C, Rokutan K, Tsuchiya T, et al. (2000) Geranylgeranylacetone protects cultured guinea pig gastric mucosal cells from indomethacin. Dig Dis Sci 45: 1674–1679.
28. Tang D, Kang R, Xiao W, Wang H, Calderwood SK, et al. (2007) The anti-inflammatory effects of heat shock protein 72 involve inhibition of high-mobility-group box 1 release and proinflammatory function in macrophages. J Immunol 179: 1236–1244.
29. Suemasu S, Tanaka K, Namba T, Ishihara T, Katsu T, et al. (2009) A role for HSP70 in protecting against indomethacin-induced gastric lesions. J Biol Chem 284: 19705–19715.
30. Matsuda M, Hoshino T, Yamashita Y, Tanaka K, Maji D, et al. (2010) Prevention of UVB radiation-induced epidermal damage by expression of heat shock protein 70. J Biol Chem 285: 5848–5858.
31. Tanaka K, Tsutsumi S, Arai Y, Hoshino T, Suzuki K, et al. (2007) Genetic evidence for a protective role of heat shock factor 1 against irritant-induced gastric lesions. Mol Pharmacol 71: 985–993.
32. Tanaka K, Namba T, Arai Y, Fujimoto M, Adachi H, et al. (2007) Genetic Evidence for a Protective Role for Heat Shock Factor 1 and Heat Shock Protein 70 against Colitis. J Biol Chem 282: 23240–23252.
33. Asano T, Tanaka K, Yamakawa N, Adachi H, Sobue G, et al. (2009) HSP70 confers protection against indomethacin-induced lesions of the small intestine. J Pharmacol Exp Ther 330: 458–467.
34. Hoshino T, Murao N, Namba T, Takehara M, Adachi H, et al. (2011) Suppression of Alzheimer's disease-related phenotypes by expression of heat shock protein 70 in mice. J Neurosci 31: 5225–5234.
35. Tanaka K, Tanaka Y, Namba T, Azuma A, Mizushima T (2010) Heat shock protein 70 protects against bleomycin-induced pulmonary fibrosis in mice. Biochem Pharmacol 80: 920–931.
36. Kim VN (2005) MicroRNA biogenesis: coordinated cropping and dicing. Nat Rev Mol Cell Biol 6: 376–385.
37. Liu G, Friggeri A, Yang Y, Milosevic J, Ding Q, et al. (2010) miR-21 mediates fibrogenic activation of pulmonary fibroblasts and lung fibrosis. J Exp Med 207: 1589–1597.
38. Namba T, Honan T, Nishimura T, Mima S, Hoshino T, et al. (2009) Up-regulation of S100P expression by non-steroidal anti-inflammatory drugs and its role in anti-tumorigenic effects. J Biol Chem 284: 4158–4167.
39. Bradford MM (1976) A rapid and sensitive method for the quantitation of microgram quantities of protein utilizing the principle of protein-dye binding. Anal Biochem 72: 248–254.
40. Chu CY, Rana TM (2006) Translation repression in human cells by microRNA-induced gene silencing requires RCK/p54. PLoS Biol 4: e210.
41. Tanaka K, Ishihara T, Azuma A, Kudoh S, Ebina M, et al. (2010) Therapeutic effect of lecithinized superoxide dismutase on bleomycin-induced pulmonary fibrosis. Am J Physiol Lung Cell Mol Physiol 298: L348–360.
42. Gridelli C, Bareschino MA, Schettino C, Rossi A, Maione P, et al. (2007) Erlotinib in non-small cell lung cancer treatment: current status and future development. Oncologist 12: 840–849.
43. Ono M, Hirata A, Kometani T, Miyagawa M, Ueda S, et al. (2004) Sensitivity to gefitinib (Iressa, ZD1839) in non-small cell lung cancer cell lines correlates with dependence on the epidermal growth factor (EGF) receptor/extracellular signal-regulated kinase 1/2 and EGF receptor/Akt pathway for proliferation. Mol Cancer Ther 3: 465–472.
44. Van Schaeybroeck S, Kyula J, Kelly DM, Karaiskou-McCaul A, Stokesberry SA, et al. (2006) Chemotherapy-induced epidermal growth factor receptor activation determines response to combined gefitinib/chemotherapy treatment in non-small cell lung cancer cells. Mol Cancer Ther 5: 1154–1165.
45. Miyata H, Sasaki T, Kuwahara K, Serikawa M, Chayama K (2006) The effects of ZD1839 (Iressa), a highly selective EGFR tyrosine kinase inhibitor, as a radiosensitiser in bile duct carcinoma cell lines. Int J Oncol 28: 915–921.
46. Moon DO, Kim MO, Lee JD, Choi YH, Lee MK, et al. (2007) Molecular mechanisms of ZD1839 (Iressa)-induced apoptosis in human leukemic U937 cells. Acta Pharmacol Sin 28: 1205–1214.
47. Li J, Karlsson MO, Brahmer J, Spitz A, Zhao M, et al. (2006) CYP3A phenotyping approach to predict systemic exposure to EGFR tyrosine kinase inhibitors. J Natl Cancer Inst 98: 1714–1723.
48. Li Y, Vandenboom TG, 2nd, Wang Z, Kong D, Ali S, et al. (2010) miR-146a suppresses invasion of pancreatic cancer cells. Cancer Res 70: 1486–1495.
49. Hurst DR, Edmonds MD, Scott GK, Benz CC, Vaidya KS, et al. (2009) Breast cancer metastasis suppressor 1 up-regulates miR-146, which suppresses breast cancer metastasis. Cancer Res 69: 1279–1283.
50. Leu JI, Pimkina J, Frank A, Murphy ME, George DL (2009) A small molecule inhibitor of inducible heat shock protein 70. Mol Cell 36: 15–27.
51. Fujibayashi T, Hashimoto N, Jijiwa M, Hasegawa Y, Kojima T, et al. (2009) Protective effect of geranylgeranylacetone, an inducer of heat shock protein 70, against drug-induced lung injury/fibrosis in an animal model. BMC Pulm Med 9: 45.

Journal of Neurochemistry JNC

JOURNAL OF NEUROCHEMISTRY | 2012 | 120 | 795–805 doi: 10.1111/j.1471-4159.2011.07567.x

ORIGINAL ARTICLE

Improvement of cognitive function in Alzheimer's disease model mice by genetic and pharmacological inhibition of the EP_4 receptor

Tatsuya Hoshino,*† Takushi Namba,† Masaya Takehara,† Naoya Murao,† Takahide Matsushima,‡ Yukihiko Sugimoto,† Shuh Narumiya,§ Toshiharu Suzuki‡ and Tohru Mizushima*†

*Faculty of Pharmacy, Keio University, Tokyo, Japan

†Graduate School of Medical and Pharmaceutical Sciences, Kumamoto University, Kumamoto, Japan

‡Graduate School of Pharmaceutical Sciences, Hokkaido University, Sapporo, Japan

§Faculty of Medicine, Kyoto University, Kyoto, Japan

Abstract

Amyloid-β peptide (Aβ), which is generated by the β- and γ-secretase-mediated proteolysis of β-amyloid precursor protein (APP), plays an important role in the pathogenesis of Alzheimer's disease (AD). We recently reported that prostaglandin E_2 (PGE_2) stimulates the production of Aβ through both EP_2 and EP_4 receptors and that activation of the EP_4 receptor stimulates Aβ production through endocytosis and activation of γ-secretase. We here found that transgenic mice expressing mutant APP (APP23) mice showed a greater or lesser apparent cognitive deficit when they were crossed with mice lacking EP_2 or EP_4 receptors, respectively. Mice lacking the EP_4 receptor also displayed lower levels of Aβ plaque deposition and less neuronal and synaptic loss than control mice. Oral administration of a specific EP_4 receptor antagonist, AE3-208 to APP23 mice, improved their cognitive performance, as well as decreasing brain levels of Aβ and suppressing endocytosis and activation of γ-secretase. Taken together, these results suggest that inhibition of the EP_4 receptor improves the cognitive function of APP23 mice by suppressing Aβ production and reducing neuronal and synaptic loss. We therefore propose that EP_4 receptor antagonists, such as AE3-208, could be therapeutically beneficial for the prevention and treatment of AD.

Keywords: Alzheimer disease, aging, infammation, memory, neurodegeneration.

J. Neurochem. (2012) **120**, 795–805.

Alzheimer's disease (AD) is the most common neurodegenerative disorder of the central nervous system and the leading cause of adult onset dementia, affecting 5% of the population over the age of 65. Pathological characters of AD are accumulation of neurofibrillary tangles and senile plaques and senile plaques are composed of amyloid-β peptides (Aβ), such as Aβ40 and Aβ42 (Mattson 2004). In order to generate Aβ, β-amyloid precursor protein (APP) is first cleaved by β-secretase and then by γ-secretase (Sisodia and St George-Hyslop 2002). Monomeric Aβ easily self-assembles to form oligomers and protofibrils, which play an important role in the induction of the neuronal and synaptic loss that results in cognitive decline (Haass and Selkoe 2007). γ-Secretase is composed of four core components, including presenilin (PS)-1 and PS-2 (Haass 2004). Early onset familial AD is linked to three genes, *app*, *ps1* and *ps2* (Haass 2004), strongly suggesting that Aβ is a key factor in the pathogenesis of AD. Consequently, cellular factors that affect the production of Aβ represent good targets for drugs to prevent or treat AD.

It has been suggested that inflammation is important in the pathogenesis of AD; chronic inflammation has been observed

Received July 28, 2011; revised manuscript received October 28, 2011; accepted October 28, 2011.

Address correspondence and reprint requests to Tohru Mizushima, Faculty of Pharmacy, Keio University, 1-5-30 Shibakoen, Minato-ku, Tokyo 105-8512, Japan. E-mail: mizushima-th@pha.keio.ac.jp

Abbreviations used: Aβ, amyloid-β peptide; AD, Alzheimer's disease; APP, β-amyloid precursor protein; COX, cyclooxygenase; CTF, C-terminal fragment; LTP, long-term potentiation; NeuN, neuronal nuclei; NSAIDs, non-steroidal anti-inflammatory drugs; PGE_2, prostaglandin E_2; PKA, protein kinase A; PS, presenilin.

in the brains of AD patients, and trauma to the brain and ischemia, both of which can activate inflammation, are major risk factors for the disease (Ikonomovic *et al.* 2004; Wyss-Coray 2006). Cyclooxygenase (COX), which exists as two subtypes, COX-1 and COX-2, is essential for the synthesis of prostaglandin E_2 (PGE_2), a potent inducer of inflammation. COX-1 is expressed constitutively, whereas COX-2 expression is induced under inflammatory conditions and is responsible for the progression of inflammation (Srinivasan and Kulkarni 1989; Smith *et al.* 1998). It has been suggested that the COX-2-mediated production of PGE_2 plays an important role in the pathogenesis of AD. For example, elevated levels of PGE_2 and over-expression of COX-2 have been observed in AD patient brains (Kitamura *et al.* 1999; Montine *et al.* 1999); the extent of COX-2 expression correlates with the degree of progression of AD pathogenesis (Ho *et al.* 2001); transgenic mice constitutively over-expressing COX-2 show aging-dependent memory dysfunction (Andreasson *et al.* 2001); PGE_2 stimulates the production of reactive oxygen species in microglia and activates β-secretase (Liang *et al.* 2005); and prolonged use of non-steroidal anti-inflammatory drugs (NSAIDs), inhibitors of COX, delays the onset and reduces the risk of AD (in t' Veld *et al.* 2001; Imbimbo *et al.* 2010). Thus, in order to identify molecular targets for the development of AD drugs, it is important to understand the molecular mechanism involved in the PGE_2-mediated progression of the disease.

We recently reported that PGE_2 stimulates the production of Aβ in cells stably expressing a form of APP with two mutations (K651N/M652L; APPsw) that elevates cellular and secreted levels of Aβ (Hoshino *et al.* 2007). Using agonists and antagonists specific for each of the four PGE_2 receptors (EP_1, EP_2, EP_3 and EP_4 receptors), we found that both EP_2 and EP_4 receptors are involved in the PGE_2-stimulated production of Aβ *in vitro* (Hoshino *et al.* 2007). With respect to the mechanism underpinning this stimulation, we also recently demonstrated that activation of the EP_2 receptor stimulates the production of Aβ through activation of adenylate cyclase, an increase in the cellular level of cAMP and activation of protein kinase A (PKA) (Hoshino *et al.* 2009). In contrast, EP_4 receptor activation causes its co-internalization with PS-1 (γ-secretase) into endosomes, a process that activates γ-secretase (Hoshino *et al.* 2009). Furthermore, we showed that deletion of the EP_2 or EP_4 receptor decreases brain levels of Aβ in transgenic mice expressing APPsw (APP23, a mouse model for AD), suggesting that EP_2 or EP_4 receptor activation stimulates the production of Aβ *in vivo* (Hoshino *et al.* 2007). These previous results suggest that EP_2 and/or EP_4 receptors could represent valuable molecular targets for the treatment of AD. However, the effect of deletion of these receptors on other AD-related phenotypes, such as neuronal and synaptic loss and cognitive deficits, has not been tested. The effect on cognitive performance is particularly important, because functional phenotypes (cognitive dysfunction) and pathological phenotypes (such as an increase in the brain level of Aβ) are not always directly linked (Roberson *et al.* 2007; Kanninen *et al.* 2009). In this study, we therefore examined the effect of EP_2 and EP_4 receptor inhibition on cognitive function in APP23 mice, revealing that genetic inhibition of the EP_4 receptor but not the EP_2 receptor not only suppresses neuronal and synaptic loss but also improves cognitive performance. Similarly, oral administration of AE3-208, an EP_4 receptor-specific antagonist, improved the cognitive function of the APP23 mice. These results suggest that the EP_4 receptor is a valuable molecular target for the development of drugs to prevent or treat AD.

Materials and methods

Materials and animals

See Appendix S1.

Morris water maze test

The Morris water maze test was conducted in a circular 90- or 150-cm diameter pool filled with water at a temperature of 22.0 + 1°C, as described previously (Kobayashi *et al.* 2000; Huang *et al.* 2006), with some minor modifications. Details are described in Appendix S1.

ELISA for Aβ and β- and γ-secretase-mediated peptide cleavage assay

Aβ40 and Aβ42 levels and β- and γ-secretase activity in the brain were determined as described previously (Hoshino *et al.* 2007). Details are described in Appendix S1.

Thioflavin-S staining and immunohistochemical and immunofluorescence analyses

Thioflavin-S staining and immunohistochemical and immunofluorescence analyses were performed as detailed in Appendix S1.

Statistical analysis

All values are expressed as the mean ± standard error of the mean (SEM). One- or two-way ANOVA followed by the Tukey test was used to evaluate differences between more than two groups. The Student's *t*-test for unpaired results was used for the evaluation of differences between two groups. Differences were considered to be significant for values of $p < 0.05$.

Results

Effect of deletion of EP_2 or EP_4 receptor on cognitive function in APP23 mice

We first used a Morris water maze to compare the spatial learning and memory of 6-month-old APPsw/EP_2−/− and APPsw/EP_4−/− mice with that of APPsw/EP_2+/+ and APPsw/EP_4+/+ mice, respectively. Mice were trained for 7 days to learn the location of a hidden platform, and the time required to reach the platform (escape latency) was

measured. As shown Fig. 1(a), APPsw/EP_2−/− mice required a longer time than APPsw/EP_2+/+ animals to reach the platform, suggesting that EP_2 receptor deletion exacerbates the cognitive deficit in the APP23 mice. In contrast, the APPsw/EP_4−/− mice tended to take less time to reach the platform than the corresponding control animals (APPsw/EP_4+/+) (Fig. 1b), suggesting that deletion of the EP_4 receptor ameliorates the cognitive deficit. These differences did not reflect differences in swimming ability, because swimming speed and the ability to locate a visible platform were similar between the groups (data not shown).

Given that the above results suggest that the EP_4 receptor may represent the better potential molecular target for the development of AD drugs, we next compared AD-related phenotypes, such as the formation of plaques and neuronal and synaptic loss, between four strains of mice (WT/EP_4+/+, WT/EP_4−/−, APPsw/EP_4+/+ and APPsw/EP_4−/−). We first repeated the Morris water maze test using 6-month-old mice, under slightly different experimental conditions (such as the size of swimming pool and tracking period). As shown Fig. 2(a), APPsw/EP_4+/+ mice required a longer time than WT/EP_4+/+ mice to reach the platform and this result is consistent with previous reports (Van Dam *et al.* 2003). Again, this difference did not reflect reduced swimming ability, as the swimming speed and the ability to locate a visible platform were similar between the four strains (data not shown). APPsw/EP_4−/− mice required a shorter time to reach the platform than APPsw/EP_4+/+ mice (Fig. 2a). Furthermore, there was no significant difference in the escape latency between APPsw/EP_4−/− and WT/EP_4+/+

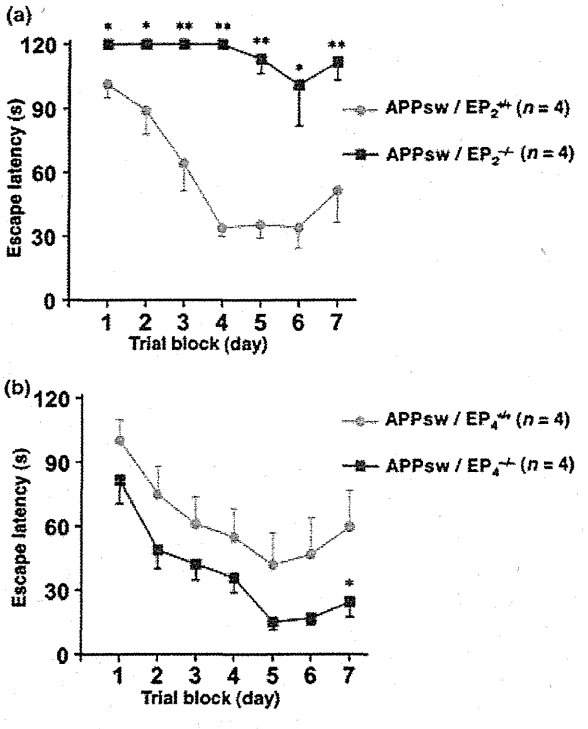

Fig. 1 Effects of deletion of the EP_2 or EP_4 receptor on spatial learning and memory in APP23 mice. Cognitive behavioral tests were carried out, using the Morris water maze, on 6-month-old APPsw/EP_2+/+ and APPsw/EP_2−/− (a) or APPsw/EP_4+/+ and APPsw/EP_4−/− (b) mice as described in the Materials and methods. Swimming paths in a circular 150-cm diameter pool were tracked for 120 s and the average (four tests) escape latency in each trial block was determined for 7 days. Values are given as mean ± SEM. Student's *t*-test: $^{**}p < 0.01$ and $^{*}p < 0.05$.

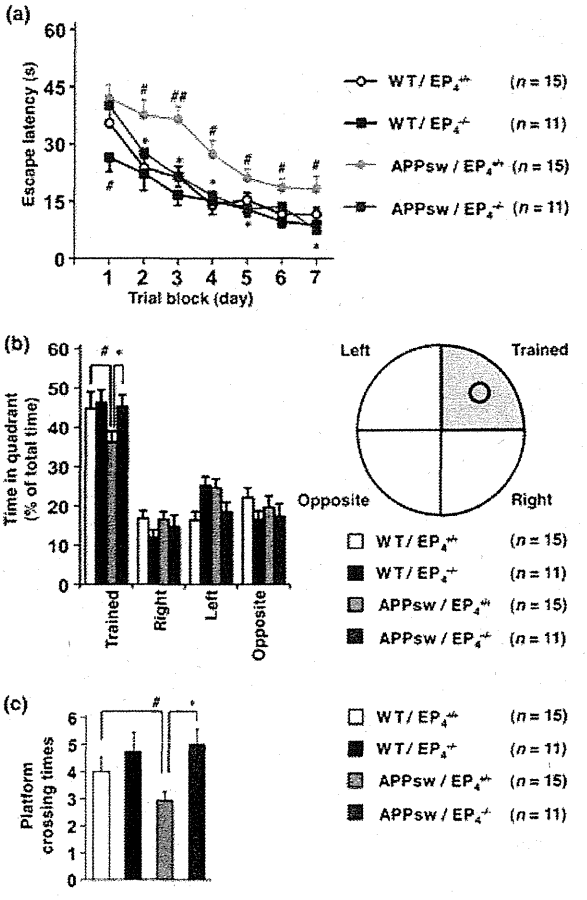

Fig. 2 Effects of deletion of the EP_4 receptor on spatial learning and memory in APP23 mice. Cognitive behavioral tests were carried out on 6-month-old WT/EP_4+/+, WT/EP_4−/−, APPsw/EP_4+/+ and APPsw/EP_4−/− mice. The swimming path in a circular 90-cm diameter pool was tracked for 60 s (a). Mice were subjected to a transfer test in which the platform was removed. The spatial memory for a platform location was estimated by per cent search time in each quadrant (the platform had been located in the 'trained' quadrant) (b) or platform crossing times (c). Values are given as mean ± SEM. One-way (b, c) or two-way (a) ANOVA followed by Tukey test: $^{*}p < 0.05$, versus APPsw/ EP_4+/+ mice; $^{\#\#}p < 0.01$ and $^{\#}p < 0.05$, versus WT/ EP_4+/+ mice.

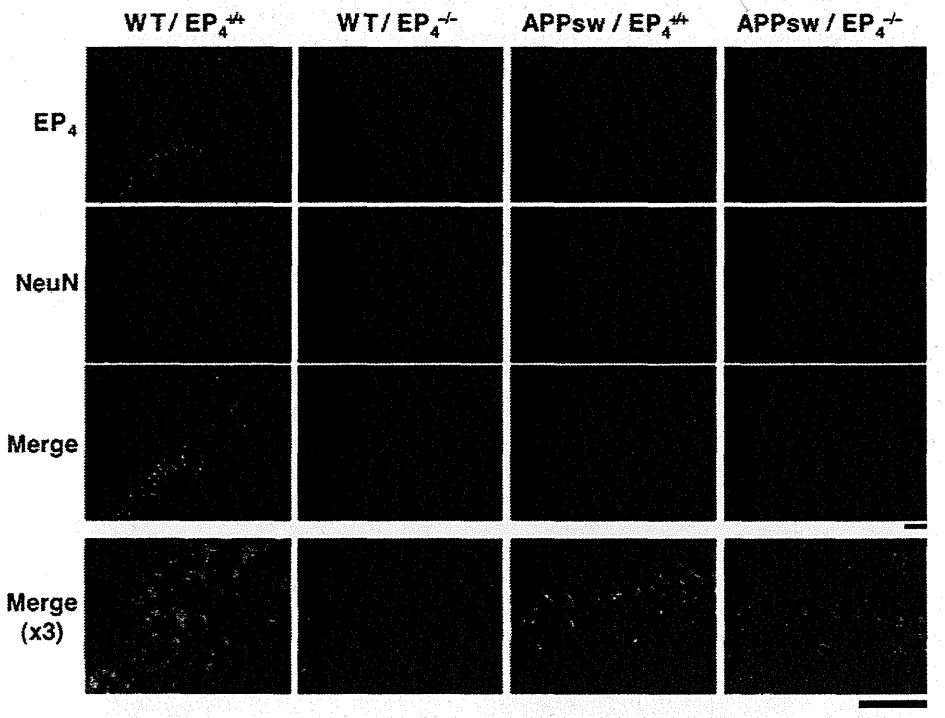

Fig. 3 EP_4 receptor expression in hippocampal neurons. Brain sections from 18-month-old WT/EP_4+/+, WT/EP_4−/−, APPsw/EP_4+/+ and APPsw/EP_4−/− mice were immunohistochemically labeled by immunofluorescence technique with antibodies against the EP_4 receptor and NeuN. The hippocampal CA3 region is shown (scale bar, 100 μm).

mice (Fig. 2a). These results suggest that the expression of APPsw disturbs spatial learning and memory and this effect can be ameliorated by deletion of the EP_4 receptor. WT/EP_4−/− mice took a significantly shorter time to reach the platform than WT/EP_4+/+ mice; however, the difference was observed only at day 0 (Fig. 2a).

We then did a transfer test to examine the spatial memory of platform location. After a 7-day training period as described above, each mouse was subjected to a Morris water maze test where the platform was removed and we measured the per cent search time for each quadrant. As shown in Fig. 2(b), the percentage of time spent in the trained quadrant was lower for the APPsw/EP_4+/+ group than for either the WT/EP_4+/+ or the APPsw/EP_4−/− mice. The crossing time of the area where the platform had been located was lower in the APPsw/EP_4+/+ group than in the WT/EP_4+/+ and APPsw/EP_4−/− cohorts (Fig. 2c). There was no significant difference between APPsw/EP_4−/− and WT/EP_4+/+ mice or between WT/EP_4−/− and WT/ EP_4+/+ mice for these indices (Fig. 2b and c). These results showed that deletion of the EP_4 receptor ameliorates the spatial memory deficits of APP23 mice.

We then examined EP_4 receptor expression in the brain of 18-month-old mice (hippocampal CA3 region) by immunofluorescence analysis. As shown in Fig. 3, expression of the receptor was clearly observed in the brains of WT/EP_4+/+ and APPsw/EP_4+/+ mice. Staining with antibody against neuronal nuclei (NeuN) confirmed expression of the EP_4 receptor in neurons (Fig. 3), consistent with previous results (Choi *et al.* 2006). However, co-staining with antibody against NeuN and that against glial fibrillary acidic protein (a maker for astrocytes) or F4/80 (a maker for microglia) was not so clear (Fig. S1).

Effect of deletion of EP_4 receptor on Aβ plaque deposition and neuronal and synaptic loss in APP23 mice

We have previously reported that the levels of Aβ40 and Aβ42 in soluble and insoluble brain fractions prepared from 6-month-old APPsw/EP_4−/− mice are lower than those from APPsw/EP_4+/+ mice (Hoshino *et al.* 2007), a finding that we confirmed here (Fig. 4a). We also examined Aβ plaque deposition by thioflavin-S staining using 18-month-old mice. As shown in Fig. 4(b) and (c), in both the hippocampus and the cerebral cortex, the level of Aβ plaque deposition was much lower in APPsw/EP_4−/− mice than in APPsw/EP_4+/+ animals.

We next determined the number of neurons in the hippocampal CA3 region by NeuN staining using 18-month-old mice. As shown in Fig. 4(d) and (e), the number of NeuN-positive cells (neurons) was significantly

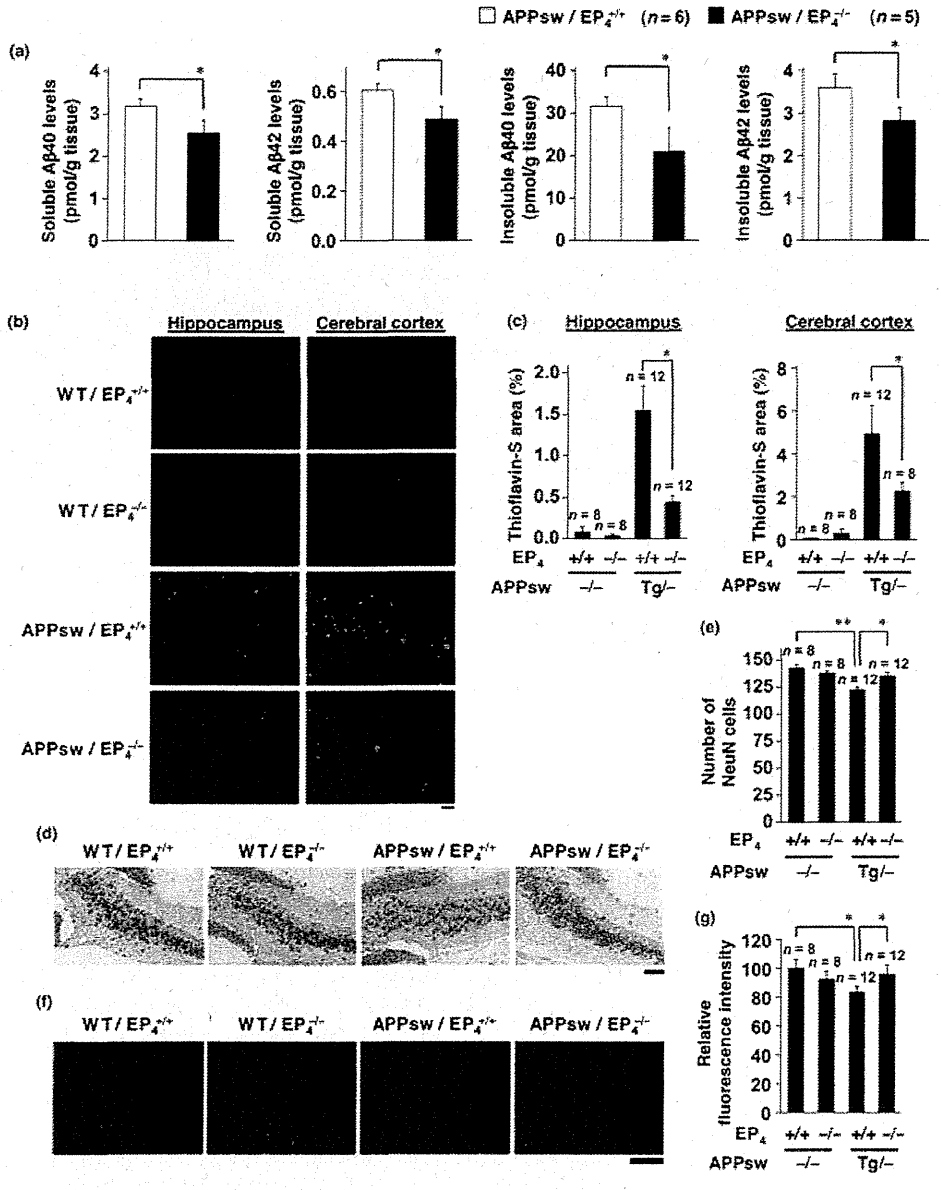

Fig. 4 Effects of EP_4 receptor deletion on Aβ levels, Aβ plaque deposition and neuronal and synaptic loss in APP23 mice. Soluble and insoluble fractions were prepared from the brains of 6-month-old APPsw/EP_4+/+ and APPsw/EP_4−/− mice. The amounts of Aβ40 and Aβ42 in each fraction were determined by ELISA as described in the Materials and methods (a). Values are given as mean ± SEM. Student's *t*-test: $^*p < 0.05$. Brain sections from 18-month-old APPsw/EP_4+/+, APPsw/EP_4−/−, WT/EP_4+/+ and WT/ EP_4−/− mice were applied to thioflavin-S staining (scale bar, 200 μm) (b) or immunohistochemical analysis with an antibody against NeuN (scale bar, 100 μm) (d) or immunofluorescence analysis with an antibody against synaptophysin (scale bar, 50 μm) (f). The relative area positive for thioflavin-S staining (c), the number of NeuN-positive cells in the hippocampal CA3 region (e) and the relative fluorescence intensity in the region (g) were determined (three sections per brain). Values are given as mean ± SEM. One-way ANOVA followed by Tukey test: $^{**}p < 0.01$; $^*p < 0.05$.

higher in the WT/EP_4+/+ and APPsw/EP_4−/− brain sections than in the APPsw/EP_4+/+ tissue, suggesting that the neuronal loss induced by Aβ was ameliorated by deletion of the EP_4 receptor. Similar results were observed for the hippocampal CA1 region (Fig. S2). We also estimated the number of synapses by synaptophysin staining using 18-month-old mice. The level of synaptophysin was higher in sections from both WT/EP_4+/+ and APPsw/EP_4−/− mice

than in those from APPsw/EP_4+/+ mice (Fig. 4f and g), indicating that Aβ-induced synaptic loss was suppressed by deletion of the EP_4 receptor. Taken together, these results suggest that deletion of the EP_4 receptor decreases the level of Aβ and Aβ plaque deposition in the brain and protects against Aβ-induced neurodegeneration. To confirm this further, stereological quantification of cell number that is more reliable should be performed in future studies.

Effect of oral administration of AE3-208 on AD-related phenotypes in APP23 mice

The results described above suggest that pharmacological inhibition of the EP_4 receptor ameliorates AD-related phenotypes in APP23 mice. In order to test this, we used an EP_4 receptor-specific antagonist, AE3-208. The K_i values of AE3-208 obtained by competition binding assay are 1.3, 30, 790 and 2400 nM for EP_4, EP_3, FP and TP, respectively, and more than 10 μM for the other prostanoid receptors (Kabashima *et al.* 2002). We have previously reported that AE3-208 suppresses the PGE_2-stimulated production of Aβ *in vitro* (Hoshino *et al.* 2007). APP23 and wild-type mice were fed either AE3-208-supplemented chow or a control diet between the ages of 3 and 6 months (the average dose of AE3-208 was calculated to be 17.8 mg/kg body weight/day). No significant differences were observed in the amount of chow consumed by the four groups of mice (APP23 or wild-type mice fed AE3-208-supplemented or control chow) during the experimental period. We then examined the spatial learning and memory of the 6-month-old animals in a Morris water maze test. Swimming speed and ability to locate a visible platform were indistinguishable between the four groups (data not shown). However, APP23 mice fed AE3-208-supplemented chow took significantly less time to find the hidden platform than the mice fed control chow (Fig. 5a). No significant difference in the escape latency was recorded between wild-type mice fed AE3-208-supplemented chow and wild-type mice fed control chow (Fig. 5a). These results suggest that the deficit in spatial learning and memory in the APP23 mice can be ameliorated by oral administration of AE3-208.

As shown in Fig. 5(b), the amount of time spent in the trained quadrant showed a tendency to be greater for the APP23 mice fed AE3-208-supplemented chow than for the mice fed control chow. Furthermore, the crossing time of the area where the platform had been located was significantly greater in the former case (Fig. 5c). However, the difference in Fig. 5(b) was not statistically significant and we have no clear explanation for the discrepancy between the 'time in quadrant' and 'platform crossings' outcomes.

In order to test whether pharmacological inhibition of the EP_4 receptor ameliorates AD-related pathological phenotypes in APP23 mice, we compared the amount of Aβ40 and Aβ42 in soluble and insoluble fractions prepared from the brains of APP23 mice fed either AE3-208-supplemented or

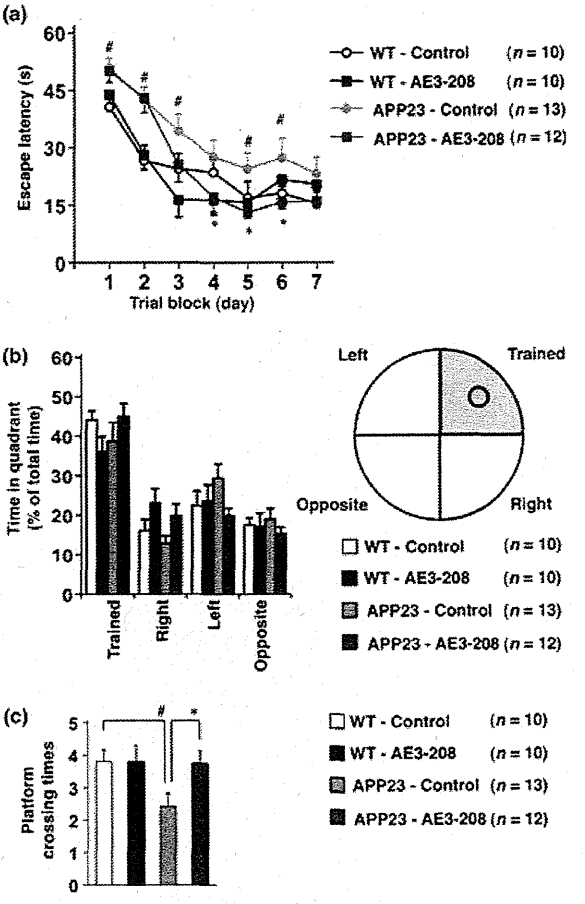

Fig. 5 Effects of oral administration of AE3-208 on spatial learning and memory in APP23 mice. Cognitive behavioral tests were carried out, using the Morris water maze, on 6-month-old wild-type mice (WT) and APP23 mice fed either AE3-208-supplemented chow (160 mg AE3-208/kg chow) or control chow between the ages of 3 and 6 months. Spatial learning and memory were tested as described in the legend of Fig. 2 (a–c). Values are given as mean ± SEM. One-way (b, c) or two-way (a) ANOVA followed by Tukey test: $^*p < 0.05$, versus APP23-control mice; $^\#p < 0.05$, versus WT-control mice.

control chow using 6-month-old mice. As shown in Fig. 6(a), the levels of Aβ40 and Aβ42 in the insoluble brain fractions from the former group were significantly lower. However, no significant difference was observed in the case of the soluble fractions (Fig. 6a).

We have previously reported that EP_4 receptor activation increases Aβ levels through its co-internalization into endosomes with PS-1 (γ-secretase), with resulting activation of γ-secretase *in vitro* (Hoshino *et al.* 2009). This finding was supported by our previous *in vivo* demonstration that brain γ-secretase activity is lower in APPsw/EP_4−/− mice than in APPsw/EP_4+/+ animals, and that the co-localization of PS-1 with Rab7 (a marker of late endosomes and

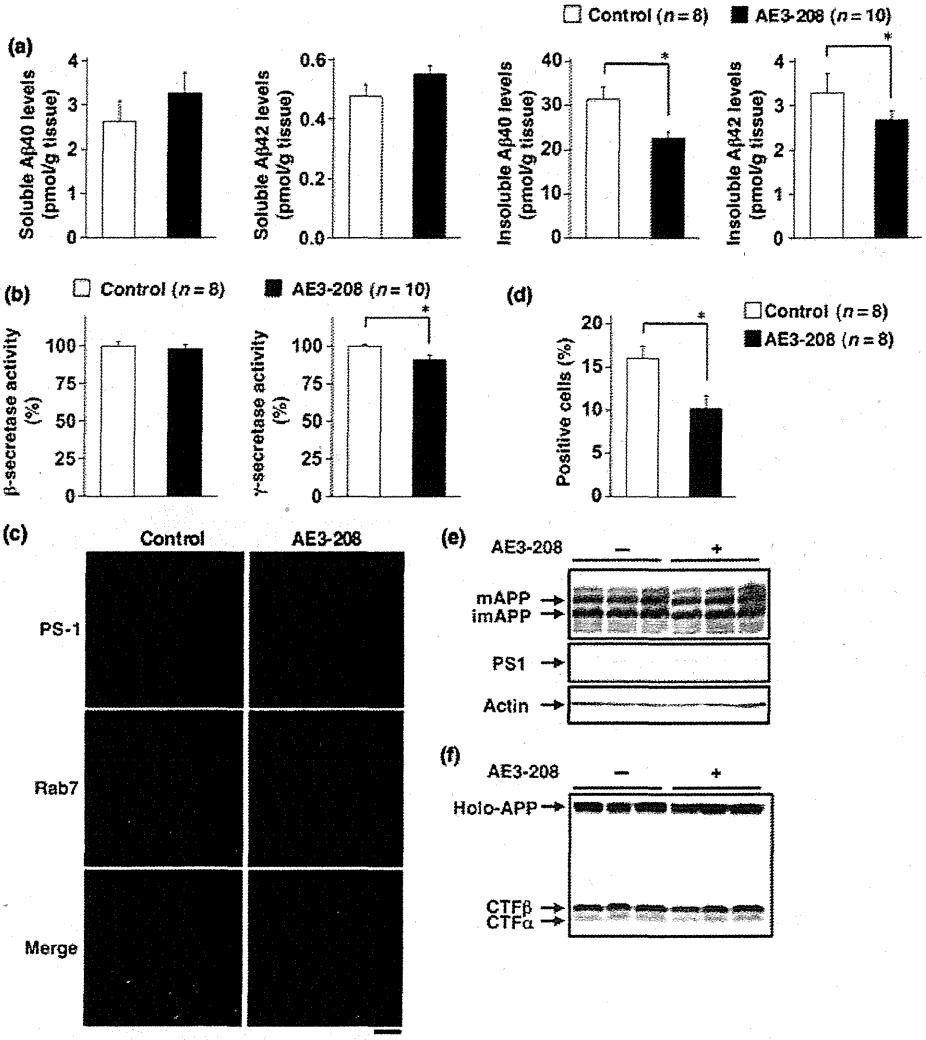

Fig. 6 Effects of oral administration of AE3-208 on Aβ levels, secretase activity, localization of γ-secretase and APP modulation in the APP23 mouse brain. APP23 mice were treated with AE3-208, as described in the legend of Fig. 5 (a–c). (6-month-old) The amounts of Aβ40 and Aβ42 were determined as described in the legend of Fig. 4 (a). Membrane fractions were prepared and subjected to a β- or γ- secretase-mediated peptide cleavage assay as described in the Materials and methods (b). Brain sections were immunostained with antibodies against PS-1 and Rab7 (scale bar, 200 μm) (c). Cells positive for both PS-1 and Rab7 staining were counted (d). Whole-cell extracts were subjected to immunoblotting with an antibody to APP (e, f), PS-1 (e) or actin (e). Values are given as mean ± SEM. Student's *t*-test: $^*p < 0.05$.

lysosomes) is not as apparent in the former group (Hoshino *et al.* 2009). In the present study, we examined the effect of oral administration of AE3-208 on the activity and localization of γ-secretase using 6-month-old mice. As shown in Fig. 6(b), the activity of γ-secretase, but not that of β-secretase, was lower in the brains of APP23 mice fed AE3-208-supplemented chow than in those of mice fed control chow. Furthermore, we found that the co-localization of PS-1 with Rab7 was not as apparent in the former group (Fig. 6c and d). We quantitatively examined the effect of AE3-208 on the expression of PS-1 staining and found that the effect was not statistically significant (data not shown).

We have previously reported that deletion of the EP_4 receptor in APP23 mice does not affect the modification of APP or α- and β-secretase activity (Hoshino *et al.* 2009), both of which are important for Aβ production. Here, we examined the effect of oral administration of AE3-208 on these processes using 6-month-old mice. We could separate by sodium dodecyl sulfate–polyacrylamide gel electrophoresis between the mature (*N*- and *O*-glycosylated) and

immature (*N*-glycosylated alone) forms of APP (mAPP and imAPP, respectively) (Tomita *et al.* 1998). As shown in Fig. 6(e), the total amount of APP and the ratio of mAPP and imAPP were similar between APP23 mice fed AE3-208-supplemented chow and those fed control chow, suggesting that the administration of AE3-208 does not affect APP modulation. We also found that the administration of AE3-208 did not affect the level of PS-1 (Fig. 6e). We then examined α- and β-secretase activity by comparing the level of secreted C-terminal fragment (CTF), representing an indirect index of secretase activity. We could not detect a CTFγ band under our experimental conditions. However, as shown in Fig. 6(f), CTFα and CTFβ were detected in the APP23 mice and the amounts of CTFα and CTFβ were indistinguishable between APP23 mice fed AE3-208-supplemented chow and those fed control chow, thereby suggesting that the administration of AE3-208 does not affect α- or β-secretase activity.

Taken together, these results suggest that the improvement in the cognitive function of the APP23 mice orally administered AE3-208 is mediated by a decrease in the brain levels of Aβ through suppression of co-internalization of the EP_4 receptor with γ-secretase into endosomes, thereby inhibiting the activation of γ-secretase.

Discussion

We have previously suggested that EP_2 and EP_4 receptors represent valuable molecular targets for the development of drugs to prevent or treat AD by showing that the amount of Aβ in the brains of APPsw/EP_2−/− and APPsw/EP_4−/− mice is lower than that in the respective control mice (Hoshino *et al.* 2007). However, among the antagonists specific for either the EP_2 or EP_4 receptor, or both, which type offers the most therapeutic potential? In order to address this issue, we herein compared the cognitive performance of APPsw/EP_2−/− or APPsw/EP_4−/− mice with that of their respective wild-type counterparts. This approach was adopted because, although AD is characterized by cognitive impairment, the functional (cognitive) phenotypes and pathological phenotypes (such as an increase in Aβ levels and Aβ plaque deposition) of the disease are not always directly linked. For example, some conditions ameliorate cognitive dysfunction in AD model mice without affecting the pathological phenotypes (Roberson *et al.* 2007; Kanninen *et al.* 2009). Our results suggested that APPsw/EP_4−/− mice but not APPsw/EP_2−/− mice display a higher level of cognitive function (spatial learning and memory) than their respective wild-type controls, suggesting that inhibition of the EP_4 receptor might prove the better therapeutic option.

We have previously reported that PGE_2-stimulated production of Aβ *in vitro* is partially mediated by EP_2 receptor-dependent activation of the cAMP–PKA pathway (Hoshino *et al.* 2009), and that the amount of Aβ in the brains of APPsw/EP_2−/− mice is lower than that in control mice (Hoshino *et al.* 2007). Another group has also shown that deletion of the EP_2 receptor in AD model mice reduces Aβ plaque deposition (Liang *et al.* 2005). Thus, it is surprising that deletion of this receptor exacerbates cognitive dysfunction in APP23 mice, suggesting that deletion of the EP_2 receptor impaired cognitive performance through an Aβ-independent mechanism. It has previously been reported that Aβ inhibits long-term potentiation (LTP) through inhibition of the cAMP–PKA pathway (Vitolo *et al.* 2002), and that inhibition of the EP_2 receptor also suppresses LTP via a similar mechanism (Akaneya and Tsumoto 2006). Thus, deletion of the EP_2 receptor may exacerbate cognitive dysfunction in APP23 mice through inhibition of LTP, a process known to be important for memory formation. It was recently reported that deletion of the gene encoding EP_2 receptor in mice without the expression of APPsw have behavioral deficits (Savonenko *et al.* 2009), thus it is unclear whether the observed effects of EP_2 receptor deletion in this study are specific to the AD model. However, it was previously reported that siRNA for EP_4 did not affect LTP (Akaneya and Tsumoto 2006).

We have previously reported that EP_4 receptor activation stimulates the production of Aβ through its co-internalization with γ-secretase into endosomes, leading to the activation of γ-secretase (Hoshino *et al.* 2009). We also showed that there are lower levels of Aβ and less endosomal localization of γ-secretase in the brains of APPsw/EP_4−/− mice than in those of APPsw/EP_4+/+ animals (Hoshino *et al.* 2007, 2009). Furthermore, in the present study, we have demonstrated that APPsw/EP_4−/− mice display lower levels of Aβ plaque formation and neuronal and synaptic loss than APPsw/EP_4+/+ mice. These results suggest that deletion of the EP_4 receptor ameliorates cognitive dysfunction in APP23 mice by decreasing brain levels of Aβ and suppressing neurodegeneration.

The findings of the present study also demonstrate that oral administration of the EP_4 receptor-specific antagonist, AE3-208, ameliorates the spatial learning and memory deficits of APP23 mice. AE3-208 has been shown to have some therapeutically beneficial effects, including suppression of tumor growth (Terada *et al.* 2010) and suppression of autoimmune encephalomyelitis (Yao *et al.* 2009). However, it has been reported that AE3-208 exacerbates dextran sodium sulfate-induced colitis, an animal model for ulcerative colitis (Kabashima *et al.* 2002), and that a specific agonist for the EP_4 receptor stimulates bone formation and prevents bone loss (Yoshida *et al.* 2002), suggesting that EP_4 receptor antagonists, including AE3-208, have adverse effects on colitis and osteoporosis, possibilities that must be considered if these agents are to be developed for the clinical treatment of AD. Although the transitional character of orally administered AE3-208 to the brain has not yet been examined, the results of the present study suggest that it can

pass the blood–brain barrier. AD is a chronic disease that requires long-term drug treatment in order to produce therapeutic effects. Thus, this property of AE3-208 would be of great advantage for its clinical use. As for the mechanism underpinning the amelioration of cognitive dysfunction in the APP23 mice following the administration of AE3-208, we believe that this is mediated by a similar mechanism to EP_4 receptor deletion, given that oral administration of AE3-208 decreases levels of Aβ and γ-secretase activity and inhibits the localization of γ-secretase in endosomes. The soluble Aβ level was reduced in APPsw/EP_4−/− mice but not in mice administered with AE3-208. This difference would be because of the difference in extent of the inhibition; deletion of the gene encoding EP_4 receptor completely inhibits the function of this protein, whereas administration of the drug may cause partial inhibition. As for the difference between soluble and insoluble Aβ for the modulation by administration of AE3-208, we have no clear explanation at present. One possible explanation is that the temporal alteration in synthesis of Aβ may affect more drastically soluble Aβ level than insoluble one.

Although this study focused on how inflammation affects the pathogenesis of AD through PGE_2 but not on how inflammation is induced in association with AD progression, we examined the effect of inhibition of EP_4 receptor on the activation of astrocytes. As shown in Fig. S3, the expression of glial fibrillary acidic protein (a maker for the activity of astrocytes) was higher in 18-month-old APPsw/EP_4+/+ mice than in WT/EP_4+/+ and APPsw/EP_4−/− mice. As for AE3-208, because we used 6-month-old mice, the activation of astrocytes by the expression of APPsw was not so clear; however, the activity was a little lower in drug-treated mice than in control mice (Fig. S3). These results suggest that the inhibition of EP_4 receptor suppresses APPsw-mediated activation of astrocytes (inflammation). Based on previously reported results, the activation of EP_4 receptor seems to affect immune systems both positively and negatively. For example, EP_4 receptor-stimulated differentiation of T_H1 cells and production of IL-23 in dendritic cells and resulting inflammation in experimental autoimmune encephalomyelitis were reported (Yao *et al.* 2009). However, in microglia, the activation of EP_4 receptor was reported to suppress the LPS-stimulated production of pro-inflammatory cytokines (Shi *et al.* 2010).

As described in the introduction, NSAIDs have attracted considerable attention as a new class of drugs for the treatment and prevention of AD, although it should also be noted that some clinical studies have recorded negative results (Imbimbo *et al.* 2010). NSAIDs can be classified into two groups: newly developed COX-2-specific NSAIDs (such as celecoxib) and classical NSAIDs without COX-2 specificity (such as indomethacin). The clinical use of classical NSAIDs is associated with gastrointestinal side effects (Hawkey 2000), as a result of the strong protective effect of prostaglandins on the gastrointestinal mucosa (Vane and Botting 1996). Given that it is mainly COX-1, which is expressed in this mucosa, COX-2-specific NSAIDs cause less of an effect on prostaglandin levels in this region, and therefore produce fewer gastrointestinal side effects than classical NSAIDs. However, it has recently been shown that clinical use of COX-2-specific NSAIDs is associated with cardiovascular thrombotic side effects (Ray *et al.* 2004; Singh 2004). These side effects of NSAIDs are likely to prove problematic if the drugs are used long term for the prevention or treatment of AD.

Compared with NSAIDs, we consider that EP_4 receptor-specific antagonists have advantages in relation to both safety and efficacy, based on the following lines of evidence. EP_1 and EP_3 receptors have been reported to be involved in PGE_2-mediated protection of the gastrointestinal mucosa by stimulating the production of bicarbonate and gastric mucosal blood flow, respectively (Takeuchi *et al.* 1997; Araki *et al.* 2000). Therefore, antagonists specific for the EP_4 receptor would be gastrointestinally safer than NSAIDs. However, it is now believed that inflammation has both positive and negative effects in relation to the progression of AD; for example, inflammation activates the phagocytosis of Aβ by microglia (Shaftel *et al.* 2007; Chakrabarty *et al.* 2010). However, NSAIDs that inhibit overall inflammation inactivate microglial phagocytosis (Yan *et al.* 2003). Therefore, compared with general anti-inflammatory agents, inhibitors that specifically act on the inflammation-mediated progression of AD may be more effective. NSAIDs suppress inflammation through both COX-dependent and COX-independent mechanisms, such as activation of the peroxisome proliferators activated receptor-γ and inhibition of nuclear factor-kB (Tegeder *et al.* 2001), with COX-mediated inhibition and the resulting decrease in PGE_2 levels seen to play a major role in the anti-AD activity of NSAIDs (Qin *et al.* 2003; Heneka *et al.* 2005). Furthermore, it was recently reported that the ability of NSAIDs to decrease PGE_2 levels is important in NSAID-dependent protection of hippocampal LTP against Aβ toxicity and restoration of Aβ-mediated suppression of synaptic plasticity and memory function (Kotilinek *et al.* 2008). Based on the findings of the present study, we consider that PGE_2 impairs cognitive performance at least partly through activation of the EP_4 receptor. Thus, we propose that EP_4 receptor-specific antagonists, such as AE3-208, will prove therapeutically more effective than NSAIDs as a result of their greater safety and efficacy. However, although we previously suggested that EP_1 and EP_3 receptors are not involved in PGE_2-stimulated production of Aβ *in vitro*, it is not clear whether activation of EP_1 and EP_3 receptors affect cognitive performance. Furthermore, modulation of COX-2 expression by activation of EP_4 receptor was also suggested (Shi *et al.* 2010). Therefore, the mechanism by which PGE_2 modulates cognitive performance is unclear at present and understanding of such mechanism is important for the identification of other targets of AD drugs.

Acknowledgements

We thank Dr M. Staufenbiel (Novartis Institutes for BioMedical Research) for providing transgenic mice. We also thank Ono Pharmaceutical Co. (Osaka, Japan) for providing AE3-208. This work was supported by Grants-in-Aid for Scientific Research from the Ministry of Health, Labour, and Welfare of Japan, as well as the Japan Science and Technology Agency, Grants-in-Aid for Scientific Research from the Ministry of Education, Culture, Sports, Science and Technology, Japan. Authors have no conflicts of interest.

Supporting information

Additional supporting information may be found in the online version of this article:

Appendix S1. Supplementary Materials and methods.

As a service to our authors and readers, this journal provides supporting information supplied by the authors. Such materials are peer-reviewed and may be re-organized for online delivery, but are not copy-edited or typeset. Technical support issues arising from supporting information (other than missing files) should be addressed to the authors.

References

Akaneya Y. and Tsumoto T. (2006) Bidirectional trafficking of prostaglandin E2 receptors involved in long-term potentiation in visual cortex. *J. Neurosci.* **26**, 10209–10221.

Andreasson K. I., Savonenko A., Vidensky S. *et al.* (2001) Age-dependent cognitive deficits and neuronal apoptosis in cyclooxygenase-2 transgenic mice. *J. Neurosci.* **21**, 8198–8209.

Araki H., Ukawa H., Sugawa Y., Yagi K., Suzuki K. and Takeuchi K. (2000) The roles of prostaglandin E receptor subtypes in the cytoprotective action of prostaglandin E2 in rat stomach. *Aliment. Pharmacol. Ther.* **14**(Suppl. 1), 116–124.

Chakrabarty P., Jansen-West K., Beccard A. *et al.* (2010) Massive gliosis induced by interleukin-6 suppresses Abeta deposition in vivo: evidence against inflammation as a driving force for amyloid deposition. *FASEB J.* **24**, 548–559.

Choi J. S., Kim H. Y., Chun M. H., Chung J. W. and Lee M. Y. (2006) Expression of prostaglandin E2 receptor subtypes, EP2 and EP4, in the rat hippocampus after cerebral ischemia and ischemic tolerance. *Cell Tissue Res.* **324**, 203–211.

Haass C. (2004) Take five-BACE and the gamma-secretase quartet conduct Alzheimer's amyloid beta-peptide generation. *EMBO J.* **23**, 483–488.

Haass C. and Selkoe D. J. (2007) Soluble protein oligomers in neurodegeneration: lessons from the Alzheimer's amyloid beta-peptide. *Nat. Rev. Mol. Cell Biol.* **8**, 101–112.

Hawkey C. J. (2000) Nonsteroidal anti-inflammatory drug gastropathy. *Gastroenterology* **119**, 521–535.

Heneka M. T., Sastre M., Dumitrescu-Ozimek L. *et al.* (2005) Acute treatment with the PPARgamma agonist pioglitazone and ibuprofen reduces glial inflammation and Abeta1-42 levels in APPV717I transgenic mice. *Brain* **128**, 1442–1453.

Ho L., Purohit D., Haroutunian V. *et al.* (2001) Neuronal cyclooxygenase 2 expression in the hippocampal formation as a function of the clinical progression of Alzheimer disease. *Arch. Neurol.* **58**, 487–492.

Hoshino T., Nakaya T., Homan T. *et al.* (2007) Involvement of prostaglandin E2 in production of amyloid-beta peptides both in vitro and in vivo. *J. Biol. Chem.* **282**, 32676–32688.

Hoshino T., Namba T., Takehara M., Nakaya T., Sugimoto Y., Araki W., Narumiya S., Suzuki T. and Mizushima T. (2009) Prostaglandin E2 stimulates the production of amyloid-beta peptides through internalization of the EP4 receptor. *J. Biol. Chem.* **284**, 18493–18502.

Huang S. M., Mouri A., Kokubo H. *et al.* (2006) Neprilysin-sensitive synapse-associated amyloid-beta peptide oligomers impair neuronal plasticity and cognitive function. *J. Biol. Chem.* **281**, 17941–17951.

Ikonomovic M. D., Uryu K., Abrahamson E. E. *et al.* (2004) Alzheimer's pathology in human temporal cortex surgically excised after severe brain injury. *Exp. Neurol.* **190**, 192–203.

Imbimbo B. P., Solfrizzi V. and Panza F. (2010) Are NSAIDs useful to treat Alzheimer's disease or mild cognitive impairment?. *Front. Aging Neurosci.* **2**, 1–14.

Kabashima K., Saji T., Murata T. *et al.* (2002) The prostaglandin receptor EP4 suppresses colitis, mucosal damage and CD4 cell activation in the gut. *J. Clin. Invest.* **109**, 883–893.

Kanninen K., Heikkinen R., Malm T. *et al.* (2009) Intrahippocampal injection of a lentiviral vector expressing Nrf2 improves spatial learning in a mouse model of Alzheimer's disease. *Proc. Natl Acad. Sci. USA* **106**, 16505–16510.

Kitamura Y., Shimohama S., Koike H., Kakimura J., Matsuoka Y., Nomura Y., Gebicke-Haerter P. J. and Taniguchi T. (1999) Increased expression of cyclooxygenases and peroxisome proliferator-activated receptor-gamma in Alzheimer's disease brains. *Biochem. Biophys. Res. Commun.* **254**, 582–586.

Kobayashi K., Noda Y., Matsushita N. *et al.* (2000) Modest neuropsychological deficits caused by reduced noradrenaline metabolism in mice heterozygous for a mutated tyrosine hydroxylase gene. *J. Neurosci.* **20**, 2418–2426.

Kotilinek L. A., Westerman M. A., Wang Q. *et al.* (2008) Cyclooxygenase-2 inhibition improves amyloid-beta-mediated suppression of memory and synaptic plasticity. *Brain* **131**, 651–664.

Liang X., Wang Q., Hand T., Wu L., Breyer R. M., Montine T. J. and Andreasson K. (2005) Deletion of the prostaglandin E2 EP2 receptor reduces oxidative damage and amyloid burden in a model of Alzheimer's disease. *J. Neurosci.* **25**, 10180–10187.

Mattson M. P. (2004) Pathways towards and away from Alzheimer's disease. *Nature* **430**, 631–639.

Montine T. J., Sidell K. R., Crews B. C., Markesbery W. R., Marnett L. J., Roberts L. J. 2nd and Morrow J. D. (1999) Elevated CSF prostaglandin E2 levels in patients with probable AD. *Neurology* **53**, 1495–1498.

Qin W., Ho L., Pompl P. N. *et al.* (2003) Cyclooxygenase (COX)-2 and COX-1 potentiate beta-amyloid peptide generation through mechanisms that involve gamma-secretase activity. *J. Biol. Chem.* **278**, 50970–50977.

Ray W. A., Griffin M. R. and Stein C. M. (2004) Cardiovascular toxicity of valdecoxib. *N. Engl. J. Med.* **351**, 2767.

Roberson E. D., Scearce-Levie K., Palop J. J., Yan F., Cheng I. H., Wu T., Gerstein H., Yu G. Q. and Mucke L. (2007) Reducing endogenous tau ameliorates amyloid beta-induced deficits in an Alzheimer's disease mouse model. *Science* **316**, 750–754.

Savonenko A., Munoz P., Melnikova T., Wang Q., Liang X., Breyer R. M., Montine T. J., Kirkwood A. and Andreasson K. (2009) Impaired cognition, sensorimotor gating, and hippocampal long-term depression in mice lacking the prostaglandin E2 EP2 receptor. *Exp. Neuro.* **217**, 63–73.

Shaftel S. S., Kyrkanides S., Olschowka J. A., Miller J. N., Johnson R. E. and O'Banion M. K. (2007) Sustained hippocampal IL-1 beta overexpression mediates chronic neuroinflammation and ameliorates Alzheimer plaque pathology. *J. Clin. Invest.* **117**, 1595–1604.

Shi J., Johansson J., Woodling N. S., Wang Q., Montine T. J. and Andreasson K. (2010) The prostaglandin E2 E-prostanoid 4 receptor exerts anti-inflammatory effects in brain innate immunity. *J. Immunol.* **184**, 7207–7218.

Singh D. (2004) Merck withdraws arthritis drug worldwide. *BMJ* **329**, 816.

Sisodia S. S. and St George-Hyslop P. H. (2002) Gamma-Secretase, Notch, Abeta and Alzheimer's disease: where do the presenilins fit in? *Nat. Rev. Neurosci.* **3**, 281–290.

Smith C. J., Zhang Y., Koboldt C. M. *et al.* (1998) Pharmacological analysis of cyclooxygenase-1 in inflammation. *Proc. Natl Acad. Sci. USA* **95**, 13313–13318.

Srinivasan B. D. and Kulkarni P. S. (1989) Inhibitors of the arachidonic acid cascade in the management of ocular inflammation. *Prog. Clin. Biol. Res.* **312**, 229–249.

Takeuchi K., Yagi K., Kato S. and Ukawa H. (1997) Roles of prostaglandin E-receptor subtypes in gastric and duodenal bicarbonate secretion in rats. *Gastroenterology* **113**, 1553–1559.

Tegeder I., Pfeilschifter J. and Geisslinger G. (2001) Cyclooxygenase-independent actions of cyclooxygenase inhibitors. *FASEB J.* **15**, 2057–2072.

Terada N., Shimizu Y., Kamba T. *et al.* (2010) Identification of EP4 as a potential target for the treatment of castration-resistant prostate cancer using a novel xenograft model. *Cancer Res.* **70**, 1606–1615.

Tomita S., Kirino Y. and Suzuki T. (1998) Cleavage of Alzheimer's amyloid precursor protein (APP) by secretases occurs after O-glycosylation of APP in the protein secretory pathway. Identification of intracellular compartments in which APP cleavage occurs without using toxic agents that interfere with protein metabolism. *J. Biol. Chem.* **273**, 6277–6284.

Van Dam D., D'Hooge R., Staufenbiel M., Van Ginneken C., Van Meir F. and De Deyn P. P. (2003) Age-dependent cognitive decline in the APP23 model precedes amyloid deposition. *Eur. J. Neurosci.* **17**, 388–396.

Vane J. R. and Botting R. M. (1996) Mechanism of action of anti-inflammatory drugs. *Scand. J. Rheumatol. Suppl.* **102**, 9–21.

in t' Veld B. A., Ruitenberg A., Hofman A., Launer L. J., van Duijn C. M., Stijnen T., Breteler M. M. and Stricker B. H. (2001) Nonsteroidal antiinflammatory drugs and the risk of Alzheimer's disease. *N. Engl. J. Med.* **345**, 1515–1521.

Vitolo O. V., Sant'Angelo A., Costanzo V., Battaglia F., Arancio O. and Shelanski M. (2002) Amyloid beta -peptide inhibition of the PKA/CREB pathway and long-term potentiation: reversibility by drugs that enhance cAMP signaling. *Proc. Natl Acad. Sci. USA* **99**, 13217–13221.

Wyss-Coray T. (2006) Inflammation in Alzheimer disease: driving force, bystander or beneficial response? *Nat. Med.* **12**, 1005–1015.

Yan Q., Zhang J., Liu H., Babu-Khan S., Vassar R., Biere A. L., Citron M. and Landreth G. (2003) Anti-inflammatory drug therapy alters beta-amyloid processing and deposition in an animal model of Alzheimer's disease. *J. Neurosci.* **23**, 7504–7509.

Yao C., Sakata D., Esaki Y., Li Y., Matsuoka T., Kuroiwa K., Sugimoto Y. and Narumiya S. (2009) Prostaglandin E2-EP4 signaling promotes immune inflammation through Th1 cell differentiation and Th17 cell expansion. *Nat. Med.* **15**, 633–640.

Yoshida K., Oida H., Kobayashi T. *et al.* (2002) Stimulation of bone formation and prevention of bone loss by prostaglandin E EP4 receptor activation. *Proc. Natl Acad. Sci.* USA **99**, 4580–4585.

Biochemical Pharmacology 83 (2012) 909–922

Contents lists available at SciVerse ScienceDirect

Biochemical Pharmacology

journal homepage: www.elsevier.com/locate/biochempharm

Purification and characterization of HSP-inducers from *Eupatorium lindleyanum*

Yasuhiro Yamashita [a,b], Tsuyoshi Ikeda [c], Minoru Matsuda [b,d], Daisuke Maji [d], Tatsuya Hoshino [b], Tohru Mizushima [a,b,*]

[a] *Department of Analytical Chemistry, Faculty of Pharmacy, Keio University, Tokyo 105-8512, Japan*
[b] *Graduate School of Medical and Pharmaceutical Sciences, Kumamoto University, Kumamoto 862-0973, Japan*
[c] *Faculty of Pharmaceutical Sciences, Sojo University, Kumamoto 862-0082, Japan*
[d] *Saishunkan Pharmaceutical Co., Ltd., Kumamoto 861-2201, Japan*

ARTICLE INFO

Article history:
Received 5 October 2011
Accepted 29 December 2011
Available online 8 January 2012

Keywords:
Heat shock protein 70
Eupalinolide
Skin photoaging
Cell death
Melanogenesis

ABSTRACT

The expression of heat shock proteins (HSPs), particularly HSP70, provides resistance to stressors. We recently reported that ultraviolet (UV)-induced melanin production and skin damage were suppressed in transgenic mice expressing HSP70 and that an extract of *Eupatorium lindleyanum* induces the expression of HSP70 in cells. Here we report the purification of eupalinolide A and B (EA and EB) from *E. lindleyanum*, and describe their actions as HSP-inducers. EA and EB both induced the expression of HSP70 in cells at concentrations that did not significantly affect cell viability. Treatment of cells with EA or EB activated heat shock factor 1 (HSF1), while the artificial suppression of HSF1 expression diminished the EA- or EB-mediated induction of HSP70 expression. Furthermore, EB inhibited the interaction between HSF1 and HSP90, which is known to inhibit the activity of HSF1. These findings suggest that EA and EB induce the expression of HSP70 *via* the activation of HSF1 by inhibiting the interaction between HSF1 and HSP90. EA and EB both induced the expression of HSP70 synergistically with other stressors. Furthermore, pre-treatment of cells with EA or EB suppressed melanin production and stressor-induced apoptosis. These effects were suppressed by the artificial suppression of HSP70 expression. *In vivo*, the percutaneous administration of EB induced the expression of HSP70 and suppressed UVB radiation-induced damage, inflammatory responses and melanin production in the skin. These results suggest that EA and EB could be beneficial for use in cosmetics and medicines as a consequence of their inhibitory action on UV-induced skin damage and melanin production.

1. Introduction

In addition to changes with aging, the skin is damaged by various environmental stressors, especially by solar ultraviolet (UV) radiation (photo-aging). UV light can be separated according to wavelength into UVA (320–400 nm), UVB (290–320 nm) and UVC (100–290 nm) [1]. As most UVC light from the sun is absorbed by the ozone layer, and the cell damaging effect of UVA is relatively weak, it seems therefore that UVB plays a central role in photo-aging [2–5].

UV-induced skin damage (such as erythema, plaque-like thickening, loss of skin tone, deep furrowing and fine wrinkle formation) is caused not only by direct damage to the skin but also indirectly *via* the induction of inflammation [6]. UV radiation also induces the development of skin cancer (photo-carcinogenesis) through DNA damage [5]. Furthermore, UV-induced skin hyper-pigmentation disorders due to abnormal melanin production cause clinical and cosmetic problems. UV-induced melanin production is mediated by a cAMP-dependent pathway in which the exposure of keratinocytes to UV light stimulates the release of signal molecules, which in turn elevate the intracellular cAMP level and induce the expression of tyrosinase [7]. Tyrosinase is a rate-limiting enzyme in melanin synthesis and its expression is positively regulated by microphthalmia-associated transcription factor (MITF) [7]. Therefore, chemicals and natural products that suppress the activity and/or expression of tyrosinase could potentially be pharmaceutically and cosmetically beneficial as hypopigmenting agents. However, the UV-induced modest production of melanin plays an important role in protecting the skin against UV-dependent damage, because melanin acts as a filter to limit the penetration of UV into the epidermis and dermis [8]. Thus,

Abbreviations: ANOVA, analysis of variance; DAPI, 4,6-diamidino-2-phenylindole dihydrochloride; DMEM, Dulbecco's modified Eagle's medium; FBS, fetal bovine serum; GAPDH, glyceraldehyde-3-phosphate dehydrogenase; GGA, geranylgeranylacetone; HSF1, heat shock factor 1; HSP, heat shock protein; IBMX, 3-isobutyl-1-methylxanthine; MITF, microphthalmia-associated transcription factor; MPO, myeloperoxidase; MTT, 3-(4,5-dimethylthiazol-2-yl)-2,5-diphenyltetrazolium bromide; NF-κB, nuclear factor kappa B; UV, ultraviolet.

* Corresponding author at: Department of Analytical Chemistry, Faculty of Pharmacy, Keio University, 1-5-30, Shibakoen, Minato-ku, Tokyo 105-8512, Japan. Tel.: +81 3 5400 2628; fax: +81 3 5400 2628.
E-mail address: mizushima-th@pha.keio.ac.jp (T. Mizushima).

0006-2952/$ – see front matter © 2012 Elsevier Inc. All rights reserved.
doi:10.1016/j.bcp.2011.12.040

to develop hypopigmenting agents (skin whitening agents) without worsening UV-induced skin damage, it is important not only to suppress melanin production but also to protect the skin from UV-induced damage.

When cells are exposed to stressors, a number of so-called stress proteins are induced that confer protection against such stressors. HSPs are representative of these stress proteins and their cellular up-regulation of expression, especially that of HSP70, provides resistance as a consequence of the HSPs' capacity to refold or degrade denatured proteins produced by stressors [9]. The induction of HSP expression by stressors is achieved at the transcription level *via* heat shock factor 1 (HSF1), a transcription factor [10]. Furthermore, the stressor-induced multistep activation of HSF1, such as phosphorylation, oligomerization to a trimeric state and re-localization into the nucleus, has been identified [11]. In addition to its cytoprotective effects, HSP70 exerts an anti-inflammatory action *via* its inhibitory effect on nuclear factor kappa B (NF-κB) [12–15]. Since stressor-induced tissue damage and inflammation are involved in various diseases, HSPs and HSP-inducers have received much attention for their therapeutic potential [11]. Geranylgeranylacetone (GGA) is a leading anti-ulcer drug on the Japanese market; it has been described as a non-toxic HSP-inducer and was recently shown to suppress inflammatory bowel disease-related experimental colitis, as well as lesions of the small intestine and pulmonary fibrosis in mice [16–20].

It is known that various HSPs are constitutively expressed in the skin and that their expression, especially that of HSP70, is up-regulated by stressors such as heat-shock and UV radiation [21,22]. While the artificial expression of HSP70 in keratinocytes and melanocytes confers protection against UV *in vitro* [21,23–26], the role of HSP70 in photo-aging *in vivo* has remained unclear. We recently showed that UV radiation-induced skin damage (such as epidermal apoptosis) and the resulting inflammatory response were suppressed in transgenic mice expressing HSP70. We also found a lower level of UV-induced DNA damage in the transgenic mice than in control wild-type mice [27]. These results suggest that the protective action of HSP70 against UV radiation-induced skin damage is mediated by processes that attenuate apoptosis, inflammation and DNA damage. We also recently reported that melanin production in cultured mouse melanoma (B16) cells was suppressed by the overexpression of HSP70 and that this suppression is mediated by the modulation of MITF activity through a direct interaction between HSP70 and MITF [28]. *In vivo*, a UV radiation-induced increase in the amount of melanin in the skin was suppressed in transgenic mice expressing HSP70 [28]. Taken together, these results suggest that HSP70 inducers could be beneficial for use in hypopigmenting cosmetics and medicines, functioning by suppressing melanin production while simultaneously protecting the skin against UV-induced damage.

We searched for HSP70 inducers from Chinese herbs and found that an ethanol extract of *Eupatorium lindleyanum* (*E. lindleyanum*) can induce expression of HSP70 in B16 cells [29]. *E. lindleyanum* has been used in China and other Asian countries as a traditional medicine for the treatment of cough, fever and tracheitis based on its anti-microbial and anti-inflammatory activities [30–32]. Furthermore, it was reported that *E. lindleyanum* contains ingredients such as volatile oils, flavonoids, alkaloids, coumarins, sesquiterpenes and esters [33], although the specific molecules responsible for the pharmacological activities of *E. lindleyanum* have not been identified. In this study, we describe our efforts to purify molecules responsible for *E. lindleyanum*'s HSP70-inducing properties. We identified two compounds, eupalinolide A and B (EA and EB), both of which are capable of inducing HSP70 expression in cells at concentrations that do not affect cell viability. Our results suggest that both EA and EB induce the expression of HSP70 *via* the activation of HSF1, and that both these compounds suppress stressor-induced apoptosis and melanin production by inducing HSP70 expression. Furthermore, *in vivo* results showed that the percutaneous administration of EB induces the expression of HSP70 and suppresses UVB-induced cell damage, inflammatory responses and melanin production in the skin, suggesting that these molecules could be beneficial for use in cosmetics and medicines.

2. Materials and methods

2.1. Materials and animals

The MCI-gel CHP20P column was from Mitsubishi Chemical (Tokyo, Japan) and Chromatorex ODS column was from Fuji Silysia Ltd. (Aichi, Japan). Optimal cutting temperature (OCT) compound was from Sakura Fintechnical (Tokyo, Japan). Dulbecco's modified Eagle's medium (DMEM) was obtained from Wako Pure Chemical Industries (Osaka, Japan). The RNeasy Fibrous Tissue Mini kit and HiPerFect transfection reagent were obtained from QIAGEN (Valencia, CA), the first-strand cDNA synthesis kit was from Takara (Shiga, Japan), and the iQ SYBR Green Supermix was from Bio-Rad Laboratories (Hercules, CA). Fetal bovine serum (FBS), 3-(4,5-dimethyl-thiazol-2-yl)-2,5-diphenyl tetrazolium bromide (MTT), menadione and 3-isobutyl-1-methylxanthine (IBMX) were from Sigma–Aldrich Co. (St. Louis, MO). Dynabeads Protein G, surface-activated Dynabeads, Lipofectamine (TM2000) and Alexa Fluor 594 goat anti-mouse immunoglobulin G were purchased from Life Technologies Co. (Carlsbad, CA). Antibodies against tyrosinase, IκB-α, lamin B and actin were obtained from Santa Cruz Biotechnology (Santa Cruz, CA) and antibody against HSP70 was from R&D Systems (Minneapolis, MN). Antibodies against HSP25, HSP47, HSP60 and HSP90 were from Enzo Life Sciences Inc. (Farmingdale, NY). Antibody against MITF was obtained from Thermo Scientific (Waltham, MA). Antiserum against HSF1 and HSP40 and the HSF1 expression vector pcDNA3.1/hHSF1 were kindly provided by Dr. Akira Nakai (Yamaguchi University) [34]. L-DOPA was from Nacalai Tesque (Kyoto, Japan). Mayer's hematoxylin, 1% eosin alcohol solution and malinol were from Muto Pure Chemicals (Tokyo, Japan). VECTASHIELD was from Vector Laboratories (Burlingame, CA). 4′,6-Diamidino-2-phenylindole (DAPI) was from Dojindo Laboratories (Kumamoto, Japan). The whole plant of *E. lindleyanum* was from Maruzen Pharmaceuticals (Hiroshima, Japan). Transgenic mice expressing HSP70 and their wild-type counterparts (6–8 weeks old, male) were a gift from Drs. C.E. Angelidis and G.N. Pagoulatos (University of Ioannina, Ioannina, Greece) and were prepared as described previously [35]. Homozygous transgenic mice were used in these experiments. The experiments and procedures described here were performed in accordance with the Guide for the Care and Use of Laboratory Animals as adopted and promulgated by the National Institutes of Health and were approved by the Animal Care Committee of Keio University and Kumamoto University.

2.2. Extraction, fractionation and identification of EA and EB

The whole plant of *E. lindleyanum* (10.1 g) was extracted three times with 100% ethanol by refluxing for 2 h and the extract was concentrated *in vacuo* to afford residues (499 mg). This extract was partitioned with 90% methanol and *n*-hexane to give two fractions (90% methanol: 318 mg, *n*-hexane: 181 mg). Most of the HSP70-inducing activity (as determined by immunoblotting analysis) was recovered in the 90% methanol fraction, which was loaded onto a polystyrene gel column (MCI-gel CHP20P column (Ø 17 mm × 100 mm)) and eluted by the stepwise addition of H_2O, 50% methanol, 100% methanol and 100% acetone. Most of the HSP70-inducing activity was recovered in the 100% methanol

fraction (120 mg), which was further separated using a Chromatorex ODS column (Ø 15 mm × 150 mm) with a stepwise elution of 50% methanol, 75% methanol and 100% methanol. The active fraction (50% methanol fraction) (120 mg) was separated by reverse-phase high performance liquid chromatography (HPLC) (Cosmosil AR-II ODS, Ø 20 mm × 250 mm) to yield EA (fraction 3, 4.6 mg, MW: 463.2) and EB (fraction 7, 4.5 mg, MW: 463.2). The structures of molecules in these fractions were identified on the basis of their NMR spectra and MS data as previously reported [33].

2.3. Cell culture

We used the PAM212 mouse squamous cell carcinoma and B16 mouse melanoma cell lines in this study. PAM212 and B16 cells were cultured in DMEM supplemented with 10% FBS, 100 U/ml penicillin and 100 μg/ml streptomycin in a humidified atmosphere of 95% air with 5% CO_2 at 37 °C. Transfection with pcDNA3.1/hHSF1 was carried out using Lipofectamine (TM2000) according to the manufacturer's protocol. Cell viability was determined by the MTT method [36]. Fluorescence-activated cell sorting analysis (FACS) for the measurement of apoptotic cells was performed as described previously [36].

2.4. siRNA targeting of genes

The siRNAs for HSF1 and HSP70 and nonspecific siRNA were purchased from Qiagen. Cells were transfected with siRNA using HiPerFect transfection reagent according to the manufacturer's instructions.

2.5. Immunoblotting analysis

Whole cell and nuclear extracts were prepared as described previously [36]. The protein concentration of each sample was determined by the Bradford method [37]. Samples were applied to polyacrylamide SDS gels and subjected to electrophoresis, after which proteins were immunoblotted with each antibody.

2.6. Determination of melanin content in vitro

The melanin content of cells was determined as described previously [38,39] with some modifications. Cells were homogenized with 1 N NaOH and the melanin content was determined by measuring the absorbance at 405 nm with a plate reader (Fluostar Galaxy; BMG Labtech, Germany).

2.7. Tyrosinase activity assay

Tyrosinase activity was assayed as described previously [40] with some modifications. Cells were washed with phosphate-buffered saline (PBS) and homogenized with 20 mM Tris/HCl (pH 7.5) buffer containing 0.1% Triton X-100. Tyrosinase activity (as indicated by oxidation of L-DOPA to DOPAchrome) was monitored as follows: cell extracts (50 μl) were mixed with 100 μl of freshly prepared substrate solution (0.1% L-DOPA in PBS) and incubated at 37 °C. The production of DOPAchrome was monitored by measuring the absorbance at 475 nm with a plate reader (Fluostar Galaxy) and corrected for the auto-oxidation of L-DOPA.

2.8. Real-time RT-PCR analysis

Real-time RT-PCR was performed as previously described [41] with some modifications. Total RNA was extracted from cells using an RNeasy kit according to the manufacturer's protocol. Samples (2.5 μg RNA) were reverse-transcribed using a first-strand cDNA synthesis kit. Synthesized cDNA was used in real-time RT-PCR (Chromo 4 instrument (Bio-Rad Laboratories)) experiments using iQ SYBR GREEN Supermix and analyzed with Opticon Monitor Software (Bio-Rad Laboratories). Specificity was confirmed by electrophoretic analysis of the reaction products and by inclusion of template- or reverse transcriptase-free controls. To normalize the amount of total RNA present in each reaction, glyceraldehyde-3-phosphate dehydrogenase (GAPDH) was used as an internal standard. Primers were designed using the Primer3 website. Mouse primers were (name: forward primer, reverse primer): *hsp25*: 5′-cctcttccctatcccctgag-3′, 5′-ttggctccagactgttcaga-3′; *hsp40*: 5′-ctccagtcacccatgacctt-3′, 5′-tgctctttccatcagggttc-3′; *hsp47*: 5′-caaccccttttgaccaagaca-3′, 5′-tgattatctcgcaccaggaa-3′; *hsp60*: 5′-cgttgccaataacacaaacg-3′, 5′-cttcaggggttgtcacaggt-3′; *hsp70.1*: 5′-tgcacttgatagctgcttgg-3′, 5′-cagtcaacgcaattaccttaagaa-3′; *hsp70.3*: 5′-ggcctgaggactgtcattatt-3′, 5′-cccacgtgcaatacacaaag-3′; *hsp90α*: 5′-aaaggcagaggctgacaaga-3′, 5′-aggggaggcatttcttcagt-3′; *hsp90β*: 5′-gcggcaaagacaagaaaaag-3′, 5′-gaagtggtcctcccagtcat-3′; *hsp70*: 5′-tggtgctgacgaagatgaag-3′, 5′-aggtcgaagatgagcacgtt-3′; *tyrosinase*: 5′-cctcctggcagatcatttgt-3′, 5′-ggttttggctttgtcatggt-3′; *tyrp1*: 5′-tggaccaatcaggagaaacc-3′, 5′-atacacggacctccaagcac-3′; *dct*: 5′-tgtgcaagattgcctgtctc-3′, 5′-agtccagtgttccgtctgct-3′; *mitf*: 5′-ctagagcgcatggactttcc-3′, 5′-acaagttcctggctgcagtt-3′; *gapdh*: 5′-aactttggcattgtggaagg-3′, 5′-acacattgggggtaggaaca-3′.

2.9. Co-immunoprecipitation assay

Immunoprecipitation was carried out as described previously [42] with some modifications. Cells were harvested, lysed with lysis buffer (10 mM Tris/HCl (pH 7.5) buffer containing 0.1% NP-40 and 150 NaCl) and centrifuged. The antiserum against HSF1 was added to the supernatants and the samples were incubated for 2 h at 4 °C with rotation. Dynabeads Protein G was added and the samples were incubated for 1 h at 4 °C with rotation. Beads were washed with lysis buffer four times and proteins were eluted by boiling in SDS sample buffer.

2.10. Preparation of EB-fixed beads and pull-down assay

Immobilization of EB to surface-activated Dynabeads was carried out according to the manufacturer's protocol. Cells were harvested, lysed and centrifuged. EB-fixed beads were added to the supernatants and the samples were incubated for 2 h at 4 °C with rotation. Beads were washed four times with the lysis buffer (see above) and proteins were eluted by boiling in SDS sample buffer.

2.11. UVB irradiation

Animals and cultured cells were exposed to UVB radiation with a double bank of UVB lamps (peak emission at 312 nm, VL-215LM lamp, Vilber Lourmat, Paris, France). The UV energy was monitored by a radiometer sensor (UVX-31, UV Products, Cambridge, UK). Animals were placed under deep anesthesia with chloral hydrate (250 mg/kg) before each irradiation. Fur was removed with electric clippers prior to the first irradiation.

2.12. MPO activity

Myeloperoxidase (MPO) activity in the skin was measured as described previously [35]. Animals were placed under deep ether anesthesia and killed. The skin was dissected, rinsed with cold saline and cut into small pieces. Samples were homogenized in 50 mM phosphate buffer and centrifuged. MPO activity was determined in 10 mM phosphate buffer with 0.5 mM *o*-dianisidine, 0.00005% (w/v) hydrogen peroxide and 20 μg of protein. MPO activity was obtained from the slope of the reaction curve, and its

specific activity was expressed as the number of hydrogen peroxide molecules converted per minute and per mg of protein.

2.13. Histological and immunohistochemical analyses

For histological examination (hematoxylin and eosin staining), skin samples were fixed in 4% buffered paraformaldehyde and embedded in paraffin before being cut into 4-μm-thick sections, which were then deparaffinized and washed in PBS. Sections were stained first with Mayer's hematoxylin and then with 1% eosin alcohol solution. Samples were mounted with malinol and inspected using a BX51 microscope (Olympus; Tokyo, Japan). Fontana-Masson staining was performed as previously described [43]. The intensity of Fontana-Masson staining in the epidermis was measured by LuminaVision (Mitani Corporation, Tokyo, Japan).

For HSP70 immunohistochemical analysis, skin tissue samples were embedded in OCT compound and cryosectioned (4-μm-thick sections). Sections were blocked with 2.5% goat serum for 10 min, incubated for 12 h with antibody against HSP70 (1:200 dilution) and finally incubated for 2 h with Alexa Fluor 594 goat anti-mouse immunoglobulin G in the presence of DAPI (5 μg/ml). Samples were mounted with VECTASHIELD and inspected using fluorescence microscopy (Olympus BX51).

2.14. Assay for melanin production in vivo

Skin reflective colorimetric measurements were assessed with a narrow-band simple reflectance meter (Mexameter MX18, Courage-Khazaka, Germany). The measurement was performed for three areas of skin, and the mean value was calculated. The measurement area was 5 mm in diameter, and the instrument was calibrated using black and white calibration plates.

2.15. Statistical analysis

All values are expressed as the mean ± standard deviation (S.D.) or standard error of the mean (S.E.M.). Two-way analysis of variance (ANOVA) followed by the Tukey test was used to evaluate differences between more than three groups. Differences were considered to be significant for values of $P < 0.05$.

3. Results

3.1. Purification of HSP-inducers from E. lindleyanum extract

As mentioned in the introduction, we recently reported that an ethanol extract of *E. lindleyanum* shows HSP-inducing activity, particularly with regard to HSP70 [29]. By partition with 90% methanol and *n*-hexane, polystyrene gel column chromatography and ODS column chromatography, we carried out the purification of molecules responsible for the HSP70-inducing activity, which was monitored by immunoblotting experiments (Fig. 1A). In the final step of the purification process, we obtained 12 fractions from HPLC experiments and examined their HSP70-inducing and cytotoxic activities (Fig. 1B). HSP70-inducing activity was recovered in fractions 3 and 7, whereas cytotoxic activity was recovered in fractions 2 and 6 (Fig. 1B). ^{3}H and ^{13}C NMR analyses were performed and the presence of EA in fraction 3 and EB in fraction 7 was identified on the basis of previously reported NMR spectra and MS data [33] (Fig. 1C). While both EA and EB were identified as major sesquiterpenes in *E. lindleyanum* [33], their biological activities have not been examined.

Considering the interesting applications that HSP-inducers could have in medicines and cosmetics, it is important that they are able to induce the expression of HSPs without decreasing cell viability. As shown in Fig. 1D, the induction of HSP70 expression in B16 cells was apparent when EA or EB was employed at a concentration of 5 μg/ml, with cell viability remaining unaffected even at concentrations as high as 10 μg/ml. On the other hand, while the ethanol extract of *E. lindleyanum* induced the expression of HSP70, there was a concomitant slight decrease in cell viability (Fig. 1D), suggesting that the cytotoxic effect of the ethanol extract is not due to EA or EB. Time-course experiments showed that the induction of HSP70 expression by EA or EB was apparent within 6 h of the beginning of incubation of B16 cells with these compounds (Fig. 1E).

The induction of HSP70 expression by both EA and EB was also observed in the mouse keratinocyte cell line (PAM212 cells), again at concentrations that did not affect cell viability (Fig. 2A).

We also examined the effect of EA and EB on the expression of HSPs other than HSP70 in PAM212 cells. Both EA and EB induced HSP25, HSP40 and HSP90 expression but not that of HSP47 or HSP60 (Fig. 2B). Similar results were observed at the mRNA level (Fig. 2C). The antibody against HSP40, HSP70 or HSP90 that was used in the experiments reported in Fig. 2B can recognize Hdj1 isoform of HSP40, both HSP70.1 and HSP70.3, or both HSP90α and HSP90β, respectively. The results presented in Fig. 2C show that expression of mRNAs corresponding to all these proteins except HSP90β was induced by EA or EB. Since it was reported that the expression of HSP25 in keratinocytes plays an important role in their differentiation [44], the results in Fig. 2B and C suggest that EA or EB could affect this process.

3.2. Mechanism for the induction of HSP70 expression by EA and EB

To understand the mechanism governing the induction of HSP70 expression by EA or EB, we first examined the contribution of HSF1 by using RNA interference. As shown in Fig. 3A, transfection of cells with siRNA for HSF1 suppressed not only the expression of HSF1 but also the EA- and EB-induced expression of HSP70, showing that HSF1 is important for this induction. We also examined the phosphorylation of HSF1 and re-localization of HSF1 into the nucleus in the presence of EA or EB. The phosphorylation of HSF1 can be detected as an upward band-shift [45,46], and treatment of cells with heat-shock caused such an upward band-shift (Fig. 3B) and an increase in HSF1 in the nuclear fraction (Fig. 3C), thus demonstrating the phosphorylation and re-localization of HSF1 into the nucleus. Although the extent to which this took place was not as clear-cut as that seen with heat-shock, phosphorylation and re-localization of HSF1 into the nucleus was also observed in cells treated with EA or EB (Fig. 3B and C). Furthermore, EA- or EB-mediated phosphorylation seems to be transient, because phosphorylation was not observed in cells treated with EA or EB for 24 h (Fig. 3A). Taken together, the results presented in Fig. 3 suggest that EA and EB induce the expression of HSP70 *via* the activation of HSF1.

HSF1 is normally maintained in a latent form by virtue of its association with HSP90 [47]. We therefore tested whether EA or EB activates HSF1 by dissociation of HSF1 from HSP90. Whole cell extracts were prepared from PAM212 cells treated with EA, EB or heat-shock, and the binding of HSP90 to HSF1 was monitored by a co-immunoprecipitation assay in which we immunoprecipitated HSF1 and looked for the presence of HSP90. In these experiments, we used PAM212 cells overproducing HSF1. The efficient precipitation of HSF1 was observed in a manner that was dependent on the overexpression of HSF1 (Fig. 4A). In control extract, HSP90 was co-immunoprecipitated; however, this co-immunoprecipitation was not observed in extracts prepared from cells treated with EA, EB or heat-shock (Fig. 4A), suggesting that these treatments inhibit the binding of HSP90 to HSF1.

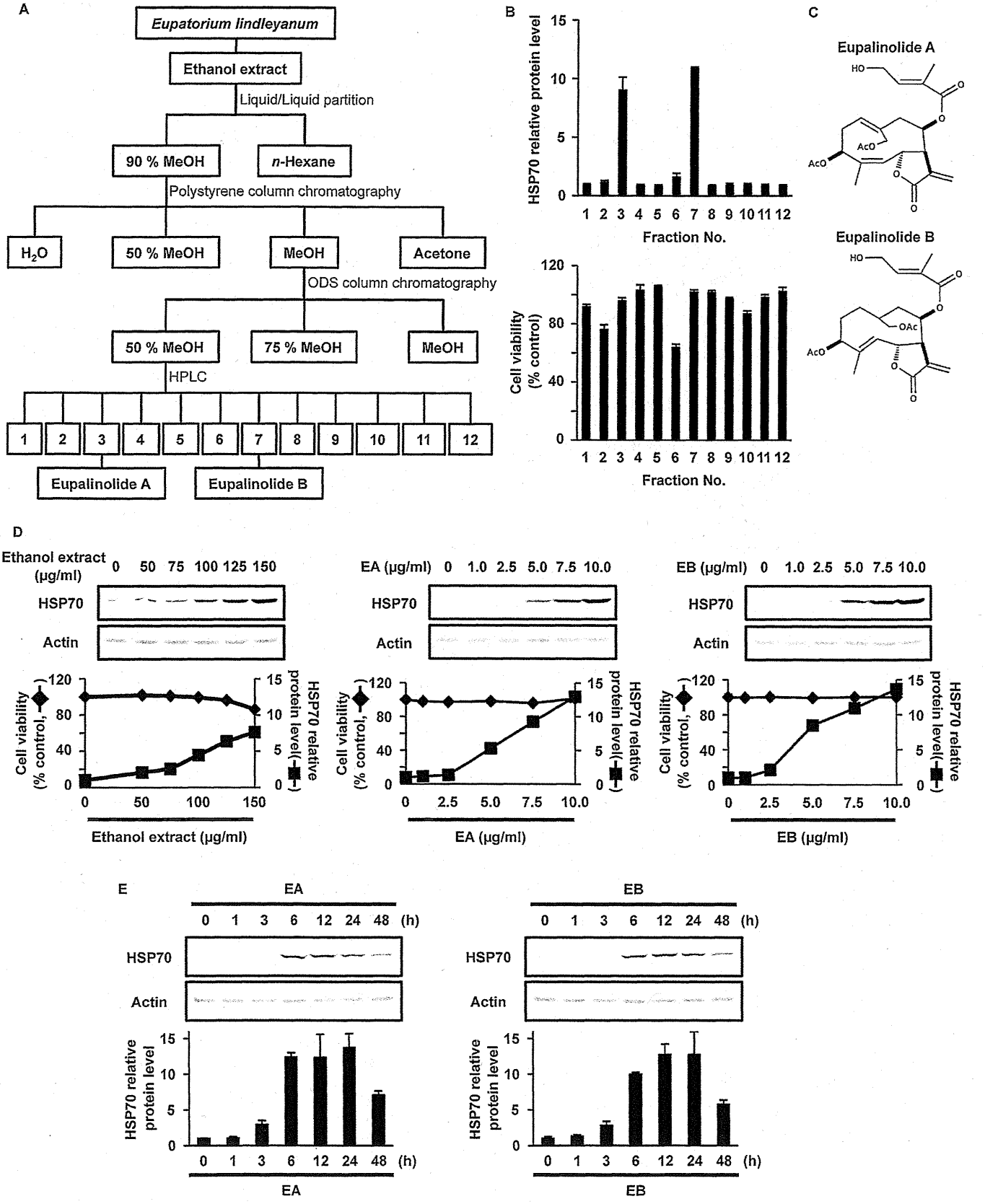

Fig. 1. Purification and characterization of EA and EB. Procedure for purification of EA and EB from *E. lindleyanum* is outlined in (A) (details are described in Section 2). B16 cells were incubated for 24 h with 7.5 μg/ml of each HPLC fraction and expression of HSP70 and cell viability were determined by immunoblotting and the MTT method, respectively (B). Structures of EA and EB are shown in (C). B16 cells were incubated with indicated concentrations of an ethanol extract of *E. lindleyanum*, EA or EB (D) or 10 μg/ml EA or EB (E) for 24 h (D) or indicated periods (E). Cell viability was determined by the MTT method and whole cell extracts were analyzed by immunoblotting with an antibody against HSP70 or actin (D and E). The intensity of the HSP70 band relative to the actin band is shown (D and E). Values are given as mean ± S.D ($n = 3$).

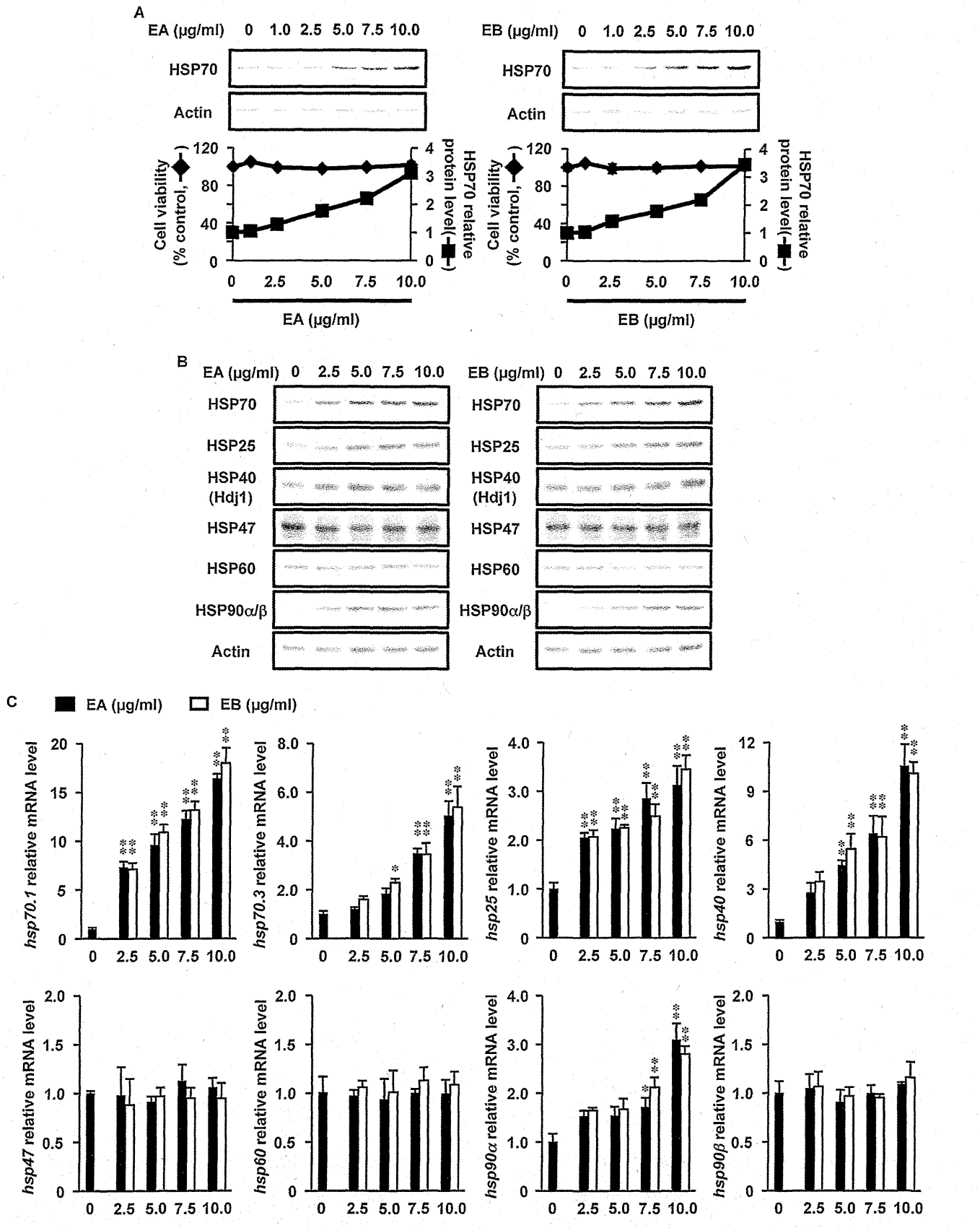

Fig. 2. Effects of EA and EB on HSP70 expression in PAM212 cells. PAM212 cells were incubated with indicated concentrations of EA or EB for 24 h (A and B) or 3 h (C). HSP70 expression and cell viability were determined as described in the legend of Fig. 1 (A). Whole cell extracts were analyzed by immunoblotting with an antibody against each protein (B). Total RNA was extracted and subjected to real-time RT-PCR using a specific primer for each gene. Values were normalized to *gapdh* gene expression and expressed relative to the control sample (C). Values are given as mean ± S.D. ($n = 3$). $^{**}P < 0.01$; $^{*}P < 0.05$.

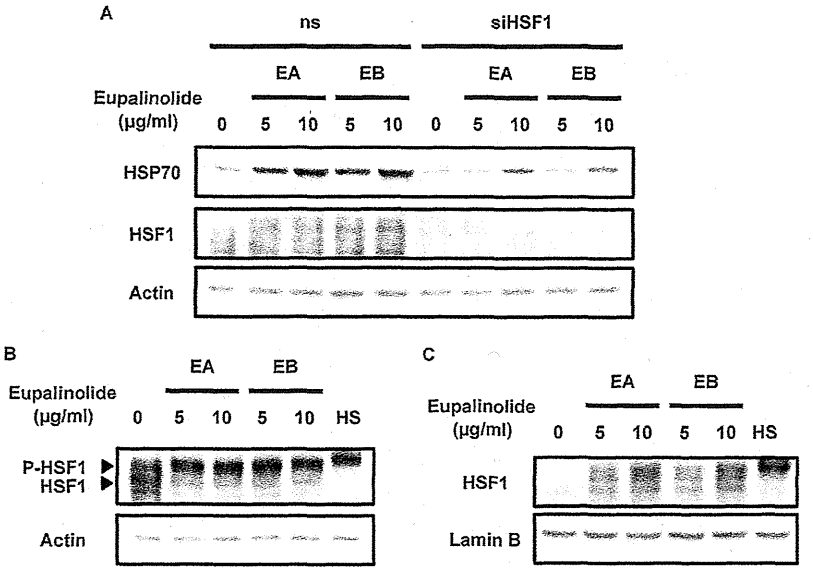

Fig. 3. HSF1 activation by EA and EB. PAM212 cells were transfected with siRNA for HSF1 (siHSF1) or nonspecific siRNA (ns) and incubated for 48 h. Cells were further incubated with indicated concentrations of EA or EB for 24 h (A). PAM212 cells were incubated with indicated concentrations of EA or EB for 3 h (B) or 1 h (C) or heat-shocked for 1 h at 43 °C (HS) (B and C). Whole cell extracts (A and B) or nuclear extracts (C) were analyzed by immunoblotting with an antibody against each protein (P-HSF1, hyperphosphorylated form of HSF1).

Finally, we tested the notion that EA or EB directly bind to HSP90 or HSF1 to inhibit their physical interaction. We prepared EB-fixed beads and after incubation of the beads with whole cell extract prepared from PAM212 cells cultured in normal conditions, collected the beads and looked for the presence of HSP90 or HSF1. As shown in Fig. 4B, HSP90 was detected in the fraction of EB-fixed beads and less clearly in that of control beads. We could not detect HSF1 in either fraction (data not shown). The detection of HSP90 in the EB-fixed bead fraction was suppressed when the incubation

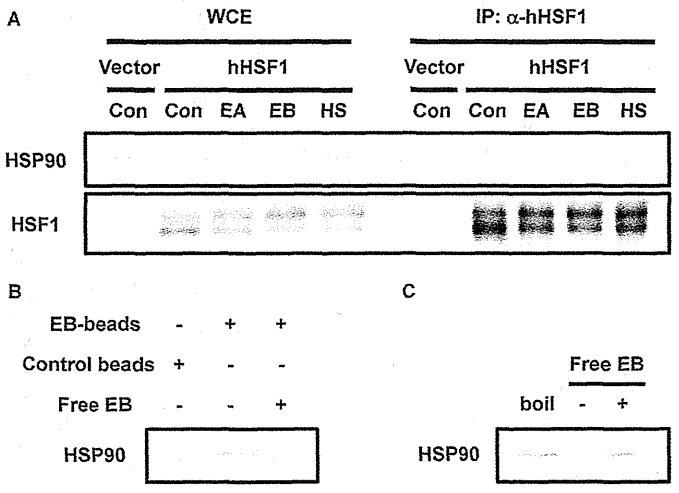

Fig. 4. Dissociation of HSF1 from HSP90 by EA and EB. PAM212 cells were transiently transfected with the expression plasmid for human HSF1 (pcDNA3.1/hHSF1) or vector (pcDNA3.1). After 24 h, cells were incubated with 5 μg/ml of EA or EB for 3 h or heat-shocked for 1 h at 43 °C (HS). Whole cell extracts (WCE) were immunoprecipitated with an antibody against HSF1 (IP: α-hHSF1) and both fractions were analyzed by immunoblotting with an antibody against each protein (A). Whole cell extracts prepared from PAM212 cells (normal culture conditions) were incubated with EB-conjugated magnetic beads (EB-beads) or control beads for 2 h in the presence or absence of free EB (0.5 mg/ml) and beads were collected. Samples were analyzed by immunoblotting with an antibody against HSP90 (B). The samples purified from whole cell extracts with EB-conjugated magnetic beads (described above) were suspended in the lysis buffer with or without free EB (0.5 mg/ml) or boiled in SDS-sample buffer. Supernatants were analyzed by immunoblotting with an antibody against HSP90 (C).

was carried out in the presence of excess amounts of free EB (Fig. 4B). Furthermore, HSP90 could be extracted from EB-fixed beads with buffer containing excess amounts of free EB but not with control buffer. The extent of extraction was similar to that achieved by boiling the beads with SDS-sample buffer (Fig. 4C). These results suggest that EB specifically binds to HSP90. We could not prepare EA-fixed beads due to the limited amount of EA available.

We also examined the synergistic effect of EA and EB with ethanol, a representative stressor that induces the expression of HSPs, on the induction of HSP70 expression. To observe the synergistic effect, a concentration of EA, EB or ethanol should be used that does not clearly induce the expression of HSP70 by itself. On this basis we used a concentration of 1–2 μg/ml for EA and EB (based on the data in Fig. 2A) or 3.5% ethanol (based on the dose-response profile of the induction of expression of HSP70 by ethanol in PAM212 cells (data not shown)). As shown in Fig. 5A and B, treatment of cells with 1–2 μg/ml EA (or EB) or 3.5% ethanol alone did not significantly up-regulate the expression of HSP70; however, a combination of both treatments clearly did induce HSP70 expression (Fig. 5A and B). Similar results were observed at the mRNA level (Fig. 5C). These results suggest that EA and EB act synergistically with other stressors such as ethanol to induce the expression of HSP70.

To examine the mechanism of this synergistic action, we examined the effect of 1–2 μg/ml EA or EB on the phosphorylation and re-localization into the nucleus of HSF1. As shown in Fig. 5D, treatment of cells with 1–2 μg/ml EA (or EB) but not 3.5% ethanol increased the phosphorylated form of HSF1, while their combined use resulted in a much higher level of phosphorylation. On the other hand, when cells were treated with 1–2 μg/ml EA (or EB) or 3.5% ethanol alone, re-localization of HSF1 into the nucleus was not stimulated; however, when they were used in combination re-localization of HSF1 into the nucleus did occur (Fig. 5E). These results suggest that the synergistic effect of EA (or EB) used in combination with other stressors to induce the expression of HSP70 is mediated by the stimulation of HSF1 phosphorylation. We also found that the simultaneous treatment of cells with EA or EB suppressed ethanol-induced cell death (Fig. 5F).

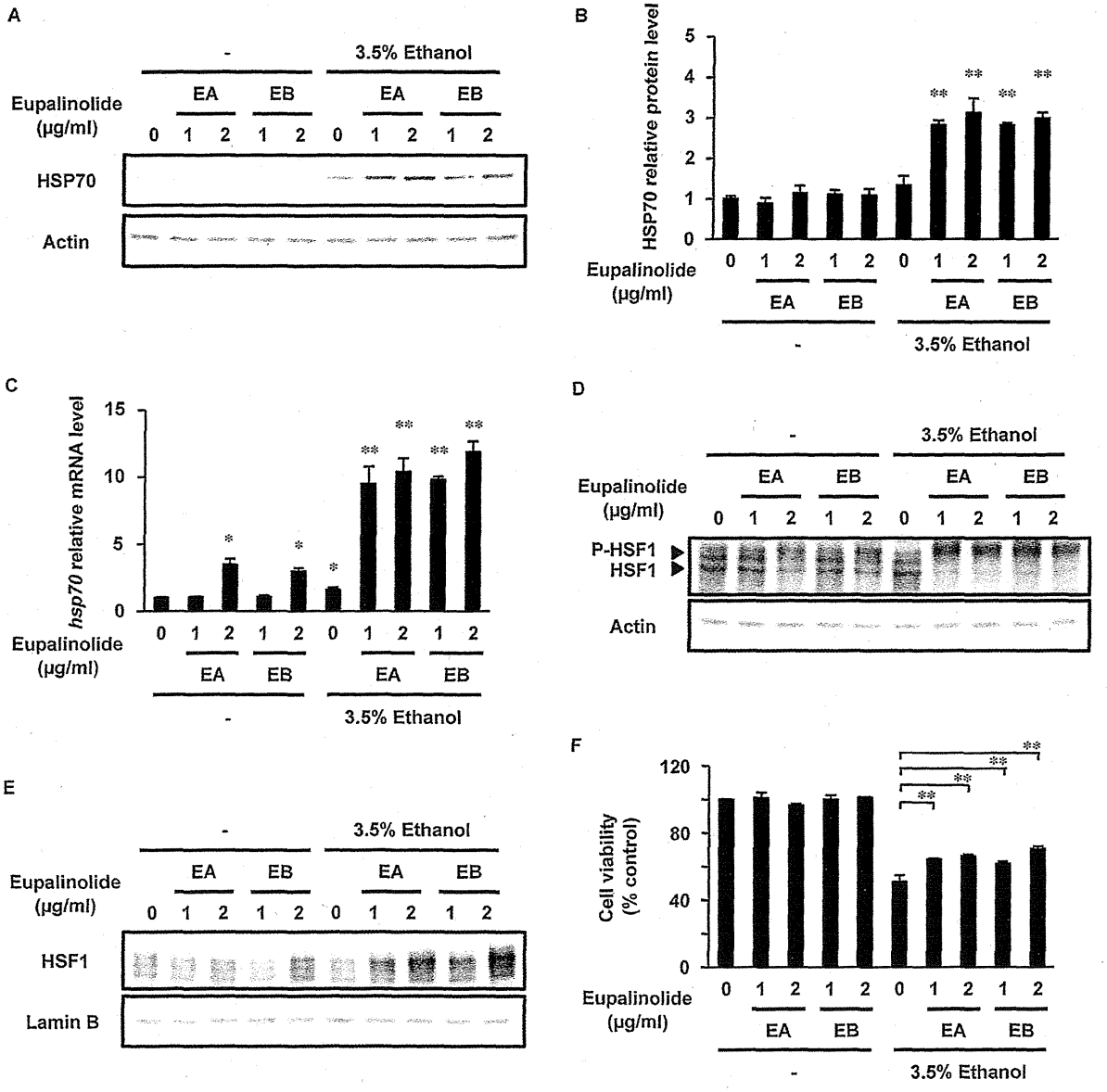

Fig. 5. Synergistic effects of EA and EB with ethanol on induction of HSP70 expression. PAM212 cells were incubated with indicated concentrations of EA or EB in the presence or absence of 3.5% ethanol for 24 h (A, B and F), 3 h (C and D) or 1 h (E). Whole cell extracts (A and D) or nuclear extracts (E) were analyzed by immunoblotting as described in the legends of Figs. 1 and 3. The intensity of the HSP70 band relative to the actin band is shown (B). The *hsp70* mRNA expression was monitored as described in the legend of Fig. 2. Cell viability was determined by the MTT method (F). Values are given as mean ± S.D. ($n = 3$). $^{**}P < 0.01$; $^{*}P < 0.05$.

3.3. Pharmacological effects of EA and EB in vitro

As mentioned above, HSP70 exerts various actions in cells, such as cytoprotection and the suppression of melanin production. Thus, as the results described above suggest that EA and EB could have pharmacological activities through the induction of HSP70 expression, we tested the cytoprotective effects and melanin inhibition properties of EA and EB. In the results of experiments shown in Fig. 6, PAM212 cells were pre-treated with EA or EB for 6 h and then exposed to various stressors. We confirmed the induction of HSP70 expression after the 6 h incubation with EA or EB in PAM212 cells (Fig. 6A). This pre-treatment with EA or EB also increased cell viability after subsequent exposure to UVB radiation (Fig. 6B). FACS analysis showed that UVB radiation induced an increase in the number of apoptotic cells (cells in sub-G1), and that this was suppressed in cells pre-treated with EA or EB (Fig. 6C). To test the contribution of HSP70 to this EA- or EB-mediated cytoprotection against UVB, we used siRNA for HSP70. Transfection of this siRNA suppressed the cytoprotective effect of EA or EB against UVB radiation but did not affect cell viability in the absence of UVB (Fig. 6D). These results suggest that EA and EB protect cells from UVB radiation *via* the induction of HSP70 expression.

We performed similar experiments for other stressors. As shown in Fig. 6E and G, pre-treatment of cells with EA or EB increased cell viability after subsequent exposure to menadione (a superoxide anion-releasing drug) or heat-shock. Furthermore, FACS analysis showed that apoptosis induced by each of these stressors was suppressed in cells pre-treated with EA or EB (Fig. 6F and H).

We then examined the effect of EA and EB on UVB-induced melanin production in B16 cells. We used IBMX (a cAMP-elevating agent that acts by inhibiting phosphodiesterase) to mimic UVB-stimulated melanin production. As shown in Fig. 7A, treatment of cells with IBMX increased the melanin content in cells, while pre-treatment of cells with EA or EB suppressed this increase in a statistically significant manner. This finding indicates that EA and EB inhibit the IBMX-stimulated production of melanin. Transfection of cells with siRNA for HSP70 suppressed the inhibitory effect